



Global Biogeochemical Cycles

RESEARCH ARTICLE

10.1002/2015GB005237

Key Points:

- Phosphorus concentrations in meltwaters are significant and higher than previously appreciated
- Ice sheet phosphorus yields are at least 10 times higher than riverine catchments
- The ice sheet plays a more important role in the Arctic phosphorus cycle than previously thought

Supporting Information:

- Text S1

Correspondence to:

J. Hawkings,
jon.hawkings@bristol.ac.uk

Citation:

Hawkings, J., J. Wadham, M. Tranter, J. Telling, E. Bagshaw, A. Beaton, S.-L. Simmons, D. Chandler, A. Tedstone, and P. Nienow (2016), The Greenland Ice Sheet as a hot spot of phosphorus weathering and export in the Arctic, *Global Biogeochem. Cycles*, 30, 191–210, doi:10.1002/2015GB005237.

Received 7 JUL 2015

Accepted 11 JAN 2016

Accepted article online 13 JAN 2016

Published online 6 FEB 2016

The Greenland Ice Sheet as a hot spot of phosphorus weathering and export in the Arctic

Jon Hawkings¹, Jemma Wadham¹, Martyn Tranter¹, Jon Telling¹, Elizabeth Bagshaw², Alexander Beaton³, Sarah-Louise Simmons¹, David Chandler¹, Andrew Tedstone⁴, and Peter Nienow⁴

¹Bristol Glaciology Centre, School of Geographical Sciences, University of Bristol, Bristol, UK, ²School of Earth and Ocean Sciences, Cardiff University, Cardiff, UK, ³National Oceanography Centre, University of Southampton, Southampton, UK,

⁴School of Geoscience, University of Edinburgh, Edinburgh, UK

Abstract The contribution of ice sheets to the global biogeochemical cycle of phosphorus is largely unknown, due to the lack of field data. Here we present the first comprehensive study of phosphorus export from two Greenland Ice Sheet glaciers. Our results indicate that the ice sheet is a hot spot of phosphorus export in the Arctic. Soluble reactive phosphorus (SRP) concentrations, up to $0.35 \mu\text{M}$, are similar to those observed in Arctic rivers. Yields of SRP are among the highest in the literature, with denudation rates of $17\text{--}27 \text{ kg P km}^{-2} \text{ yr}^{-1}$. Particulate phases, as with nonglaciated catchments, dominate phosphorus export ($>97\%$ of total phosphorus flux). The labile particulate fraction differs between the two glaciers studied, with significantly higher yields found at the larger glacier (57.3 versus $8.3 \text{ kg P km}^{-2} \text{ yr}^{-1}$). Total phosphorus yields are an order of magnitude higher than riverine values reported in the literature. We estimate that the ice sheet contributes $\sim 15\%$ of total bioavailable phosphorus input to the Arctic oceans ($\sim 11 \text{ Gg yr}^{-1}$) and dominates total phosphorus input (408 Gg yr^{-1}), which is more than 3 times that estimated from Arctic rivers (126 Gg yr^{-1}). We predict that these fluxes will rise with increasing ice sheet freshwater discharge in the future.

1. Introduction

Phosphorus (P) is a bioessential macronutrient [Ruttenberg, 2014]. The supply of P is known to influence ecosystem productivity and biogeochemical cycles in marine and terrestrial ecosystems. It is believed to be the ultimate limiting nutrient on geological timescales, in part because it cannot be fixed from the atmosphere [Broecker and Peng, 1982; Elser *et al.*, 2007; Ruttenberg, 2014; Tyrrell, 1999] and may currently be a limiting nutrient in some regions [Wu *et al.*, 2000]. Many aspects of the current global P cycle are poorly understood [Filippelli, 2008], especially terrestrial fluxes of P to the oceans, the principal speciation of P exported and the associated bioavailability of fluxes [Slomp, 2011].

Studies of the transport of P to the ocean have so far focused on riverine runoff, atmospheric deposition, and submarine groundwater discharge. Of these, riverine runoff is the dominant flux [Meybeck, 1982; Moore *et al.*, 2013; Ruttenberg, 2014; Slomp, 2011]. Recent research indicates that glaciers and ice sheets export large quantities of nutrients, such as Fe, N, and dissolved organic carbon, to downstream ecosystems [Bhatia *et al.*, 2013; Death *et al.*, 2014; Hawkings *et al.*, 2015, 2014; Hood *et al.*, 2015, 2009; Lawson *et al.*, 2014; Raiswell and Canfield, 2012; Schroth *et al.*, 2014]. Only two studies have suggested a role for glaciers in the global P cycle [Föllmi *et al.*, 2009; Hodson *et al.*, 2004]. These have focused on small glacial systems, which may have lower chemical weathering intensities than larger ice sheet catchments [Wadham *et al.*, 2010]. To date, ice sheets have largely been overlooked as P sources to the oceans.

The Greenland Ice Sheet (GrIS) is the second largest ice sheet on Earth, covering an area of approximately $1.7 \times 10^6 \text{ km}^2$ [Knight, 1999]. From 2000 to 2010, it discharged $\sim 1000 \text{ km}^3$ of freshwater ($\sim 40\%$ as runoff and $\sim 60\%$ as solid ice) into the surrounding oceans each year [Bamber *et al.*, 2012; Tedesco *et al.*, 2013]. This is likely to increase with climatic warming [Fettweis *et al.*, 2013].

Two distinct environments likely dominate phosphorus export from the GrIS. The surface is the principal source of snow and ice melt. These are relatively dilute, containing only low concentrations of rock-derived nutrients, including P. Habitats associated with supraglacial debris, including cryoconite holes, may recycle and export nutrients [Bagshaw *et al.*, 2013; Stibal *et al.*, 2009; Telling *et al.*, 2014, 2012]. The supraglacial environment plays a critical role in ice sheet hydrology as the majority of meltwater is generated at the

©2016. The Authors.

This is an open access article under the terms of the Creative Commons Attribution License, which permits use, distribution and reproduction in any medium, provided the original work is properly cited.

Table 1. Leverett Glacier (LG) and Kiattuut Sermiat Glacier (KS) Geophysical Parameters^a

	2012	2013	KS:LG
	LG	KS	
Geographical position	67.06°N, 50.17°W	61.21°N, 45.33°W	
Geology	Orthogneiss and granite	Granite, with diorite-/pyroxene-biotite, and basaltic intrusions	
Area (approximately, km ²)	600	36	0.06
Length (approximately, km)	80	16	0.20
Mean Q (m ³ s ⁻¹)	214	25	0.12
Total Q (km ³)	2.2	0.22	0.10
Specific Q (m a ⁻¹)	3.7	6.1	1.65
Mean SusSed (g L ⁻¹)	1.1	0.11	0.10
Total SusSed (kT)	2277	24.9	0.01
Sediment yield (T km ⁻²)	3795	692	0.18
Erosion rate (mm a ⁻¹) ^b	1.4	0.3	0.19
Qwt EC (μS cm ⁻¹)	8.5	26.6	3.13

^a Q = discharge; Qwt = discharge weighted; SusSed = suspended sediment; KS:LG = ratio of two glaciers in this study.

^bMean density of gneiss (2.8 T m⁻³) used for LG and granite (2.7 T m⁻³) for KS. Calculations as per Cowton *et al.* [2012].

surface and routed to the bed [Bartholomew *et al.*, 2010, 2011; Chandler *et al.*, 2013; Chu, 2014; Cowton *et al.*, 2013; Sole *et al.*, 2011]. The second source of P from the GrIS is the subglacial environment. A drainage system similar to that found under temperate glaciers is believed to be present [Bartholomew *et al.*, 2010; Chandler *et al.*, 2013; Chu, 2014; Sole *et al.*, 2011], and the environment is characterized by high rock-water ratios and microbially mediated chemical weathering of ground bedrock [Tranter *et al.*, 2002]. Meltwater drainage through the subglacial system adds solutes to waters and is thought to be an important source of nutrients [Hawkins *et al.*, 2015]. Periodic flushing of concentrated stored waters by supraglacial lake drainage events has been observed [Bartholomew *et al.*, 2011], and meltwaters emerging from beneath the ice sheet carry large quantities of fine-grained suspended sediment with concentrations $>1\text{ g L}^{-1}$ [Cowton *et al.*, 2012]. These sediments have been demonstrated to carry labile nutrients [Hawkins *et al.*, 2015, 2014; Lawson *et al.*, 2014; Schroth *et al.*, 2014].

This study investigates the importance of the GrIS in the P cycle. Hydrological and geochemical data are presented from a large ($\sim 600\text{ km}^2$) and a small ($\sim 36\text{ km}^2$) GrIS catchment of similar geology. We utilize high-resolution hydrological data sets alongside seasonal time series of dissolved and sediment-bound P species. We aim to (i) present the seasonal variation of P concentrations, (ii) determine the principal processes influencing the P concentrations, (iii) calculate P denudation rates to assess the intensity of glacial P weathering, and (iv) evaluate the importance of the ice sheet on the Arctic P cycle.

2. Methods

2.1. Study Areas

Leverett Glacier (LG; 67.06°N, 50.17°W; Table 1 and Figure 1a) is a large polythermal-based, land-terminating outlet of the GrIS. The glacier stretches ~ 80 km from the ice sheet margin and has a hydraulically active catchment area of $>600\text{ km}^2$ [Cowton *et al.*, 2012; Palmer *et al.*, 2011]. Mean annual summer discharge (2009–2012) ranged from ~ 110 to $200\text{ m}^3\text{ s}^{-1}$ and annual specific discharge of 1.8–3.7 m. Runoff from LG feeds a large glacial river system (Watson River), which discharges into the Davis Strait via Søndre Strømfjord. The catchment bedrock is composed predominantly of ancient crystalline gneiss/granite, which is the dominant geology underlying the GrIS [Henriksen *et al.*, 2009]. Hydrology is similar to temperate glaciers, with supraglacial meltwater input driving subglacial drainage evolution over the melt season, from a slow, inefficient distributed system to an efficient channelized system [Chandler *et al.*, 2013]. LG was sampled during the record GrIS ablation season of 2012 (11 May to 21 July).

Kiattuut Sermiat (KS; 61.2°N, 45.3°W; Table 1 and Figure 1b) is a smaller coastal glacier on the southern tip of the GrIS. It is also believed to have a polythermal basal regime. KS covers an estimated 36 km^2 , is around 16 km in length, and terminates in a proglacial lake. Mean ice velocity is $<60\text{ m yr}^{-1}$ and at least the final few hundred meters of ice is believed to be static ("dead ice") [Rignot and Mouginot, 2012]. Mean annual

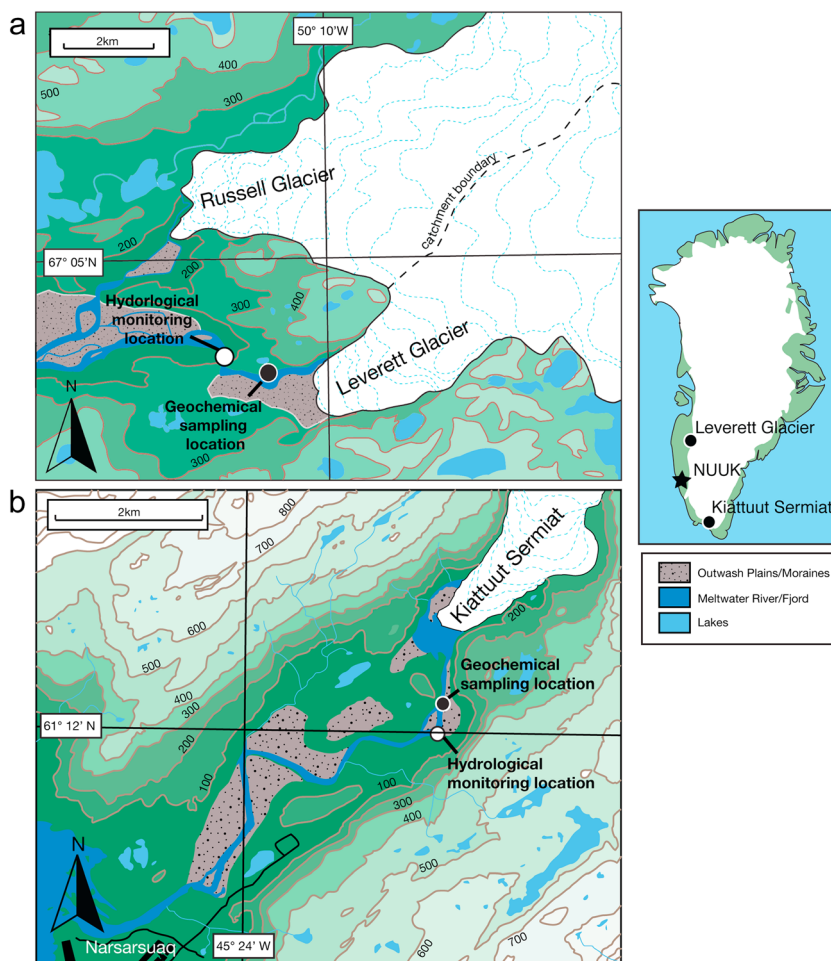


Figure 1. (a) Location of Leverett Glacier with sampling/monitoring sites from *Hawkins et al. [2014]*. Adapted from a 1:100,000 map. (b) Location of Kiattut Sermiat with sampling location and hydrological monitoring site. Adapted from a 1:50,000 map. Geographical location of study sites is shown on the map of Greenland.

summer discharge was $\sim 25 \text{ m}^3 \text{ s}^{-1}$, and specific annual discharge was 6.1 m in 2013 (Table 1). Regional geology is crystalline granite, broadly similar in composition to LG. Smaller complexes of diorite and pyroxene-biotite monzonite and basaltic intrusions are also present [*Henriksen et al., 2009*]. KS was sampled during the 2013 ablation season (21 April to 11 August).

2.2. Hydrological Monitoring

LG and KS meltwater rivers were monitored for discharge, suspended sediment concentrations, and electrical conductivity (EC) at stable bedrock sections (Figure 1) using methods previously described by *Bartholomew et al. [2011]* (Text S1 in the supporting information). pH was recorded manually when samples were taken using a handheld Hanna® HI9124 meter with standard glass electrode probe at LG and continuously using an ISFET (ion-selective field-effect transistor) Honeywell Durafet® pH sensor at KS. Handheld meters were calibrated daily using National Institute of Standards and Technology-certified pH 7 and 10 buffers (Fisherbrand™), and the ISFET sensor was calibrated monthly with low ionic strength pH 4.01 and pH 6.96 buffers (Reagecon). Errors are estimated at ± 0.05 pH units.

2.3. Sample Collection, Processing, and Storage

Bulk runoff samples were collected at least once daily during the 2012 (LG) and 2013 (KS) ablation seasons (Figure 1). Collection time was between 10.00 and 12.00 h, and on occasion between 18.00 and 19.00 h. Meltwater was collected in 2 L high-density polyethylene (HDPE) Nalgene® bottles. Samples for dissolved P

analysis were immediately filtered through a 47 mm 0.45 μm cellulose nitrate filter (Whatman[®]), mounted onto a polyethersulfone filter unit (Nalgene[®]) at LG, or a 0.45 μm Whatman[®] GD/XP PES syringe filter using a PP/PE syringe at KS (Cyanmar[®]). Filtration was carried out in a designated “clean” sampling tent (LG), or immediately on site (KS; weather permitting). Three replicate samples collected at LG using the filter unit and syringe filter methods showed no significant difference in final measured concentration ($\pm 3.6\%$). Supraglacial meltwater samples at KS were collected in a similar manner. Dissolved P samples were stored in clean 30 mL HDPE bottles (Nalgene[®]), three times rinsed with filtered sample water, and stored frozen and in the dark at -10°C , using portable field freezers, before transport back to Bristol, where they were kept at -25°C prior to analysis. Freezing is an effective and commonly used preservation method for storing low-level nutrient samples for short periods [Dore *et al.*, 1996]. Samples for suspended sediment-bound P fractions were collected from the same bulk meltwater samples. Around 200–1000 mL of meltwater was filtered through a 47 mm 0.45 μm cellulose nitrate filter (Whatman[®]), with the sediment retained and stored frozen until analysis.

2.4. Analytical Procedures

2.4.1. Dissolved Phosphorus

Soluble reactive phosphorus (SRP, also often referred to as dissolved inorganic phosphate) was determined on a LaChat QuickChem[®] 8500 series 2 flow injection analyzer (FIA; QuickChem[®] Method 31-115-01-1-I). Measurements were based on the molybdenum blue method. Precision was $\pm 3.2\%$ (LG; $n = 5$) and $\pm 2.9\%$ (KS; $n = 7$), and accuracy was $+1.5\%$ (LG) and -5.7% (KS), as determined from comparison with gravimetrically diluted 1000 mg L⁻¹ PO₄³⁻ certified stock standards (Sigma TraceCERT[®]). Field blanks were below the limit of detection (LoD), 0.01 μM ($n = 9$).

Dissolved organic phosphorus (DOP) was determined by subtracting measurements of SRP from total dissolved P. Total dissolved P was determined using the same FIA method as for SRP (Method 31-115-01-3-F), but with samples having undergone an additional sulfuric acid/persulfate digestion step at 120°C [Grasshoff *et al.*, 1999]. Digestion checks of sodium pyrophosphate (>90% recovery; $n = 5$) and sodium tripolyphosphate (>95% recovery; $n = 5$) were used to confirm method efficiency. Precision was $\pm 1.4\%$ (LG; $n = 5$) and $\pm 6.7\%$ (KS, $n = 5$), with an accuracy of -3.4% (LG) and $+2.4\%$ (KS), as determined by comparison with a gravimetrically diluted 1000 mg L⁻¹ PO₄³⁻ certified stock standard (Sigma TraceCERT[®]). Field blanks were below the LoD of 0.02 μM ($n = 9$).

2.4.2. Particulate Phosphorus

A four-step sequential extraction methodology, adapted from Stibal *et al.* [2008], was used. This method removes increasingly unreactive, operationally defined, P phases. Sediment was removed carefully by gentle scraping from air-dried filter membranes. Approximately 50 mg of sediment was added to a 2 mL PP microcentrifuge tube. Extraction 1 removes highly labile, “loosely adsorbed” P (MgCl₂-P). A 1 M MgCl₂ solution (1.5 mL) was added to the microcentrifuge tube, to give a final solution:sediment ratio similar to that used by others [Hodson *et al.*, 2004]. The tubes were placed on a reciprocating shaker for 16 h, centrifuged at 3000 rpm for ~ 10 min, and the supernatant extracted and filtered into a clean 2 mL centrifuge tube using a 1 mL syringe (PP/PE) and a 0.45 μm Whatman[®] Puradisc syringe filter (PP membrane). The sediment was subsequently shaken with 1.5 mL of Milli-Q water for 2 h, the supernatant extracted, filtered as above, and added to the initial extract. Extraction 2 removes Fe- and Al-bound P, which is believed to be moderately labile (NaOH-P). As this phase is calibrated to the growth of algae cultures, it is often referred to as “algal available” [Dorich *et al.*, 1985]. 1.5 mL of 0.1 M NaOH was added to the retained sediment, and the same process as per extraction 1 was followed. Extraction 3 removes Ca- and Mg-bound P, which is more refractory and less reactive (HCl-P). Samples were treated as above, but with a 1 M HCl solution added to the retained sediment. The final extraction, extraction 4, was used to determine “residual” and organic-bound P (Res-P). The remaining sediment was transferred to a 10 mL glass digestion tube, to which 5 mL of a sulfuric acid/potassium persulfate solution was added [Jeffries *et al.*, 1979]. Samples were autoclaved for 30 min at 120°C and 100,000 Pa, allowed to cool, and then filtered into clean PP microcentrifuge tubes as above. Samples were kept refrigerated at $<4^\circ\text{C}$ for no longer than 24 h prior to analysis. Solutions were analyzed using the SRP method described in section 2.4.1 with matrix-matched standards. Precision was found to be $\pm 0.7\%$, $\pm 0.9\%$, $\pm 0.2\%$, and $\pm 0.2\%$, and accuracy was $+0.2\%$, -0.4% , $+2.3\%$, and -2.3% based on six replicate standards for extractions 1, 2, 3, and 4, respectively. All extractions were diluted with Milli-Q water before analysis to bring them within the instrumental determination range. Extraction 1 was diluted 1:3, extraction 2 1:10, extraction 3 1:100, and extraction 4 1:15. Dry weight corrections were made based on the mean dry weight corrections of six sediment samples from LG ($\pm 3.9\%$) and twenty one samples from KS ($\pm 3.6\%$).

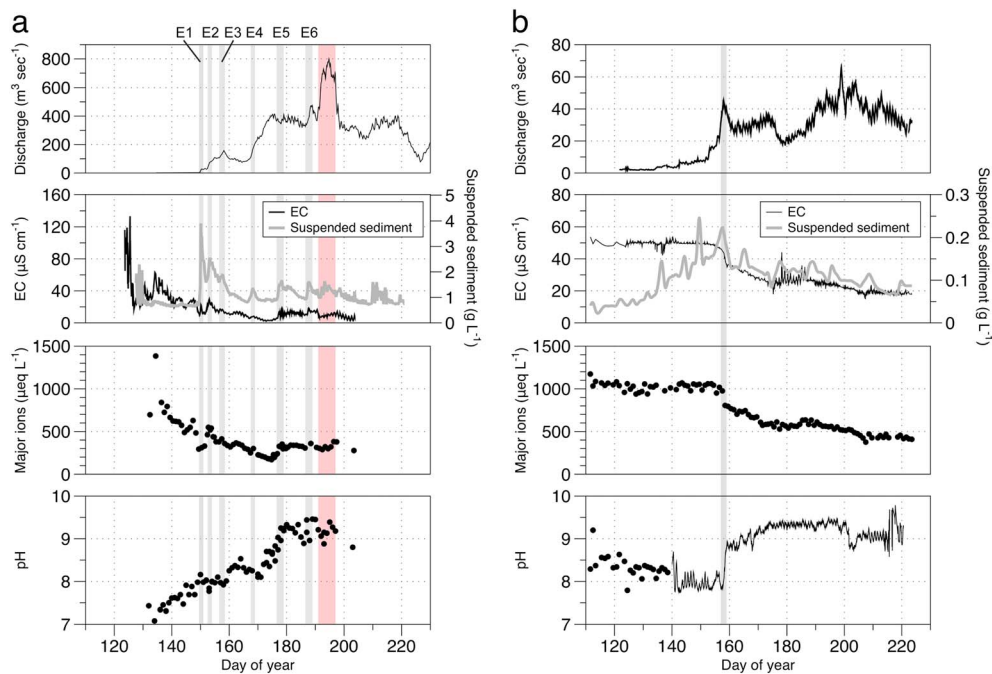


Figure 2. Hydrological and geochemical data for (a) Leverett Glacier and (b) Kiattuut Sermiat. Grey shaded areas in Figure 2a are indicative of outburst events (E) and in Figure 2b of a significant hydrological shift in the glacial drainage system (a “spring event”). The red shaded area in Figure 2a highlights the 2012 record melt event.

2.5. Principle Components Analysis

Principle components analysis (PCA) was performed using SPSS® Statistics software (IBM®). PCA is a data transformation technique used to reveal underlying relationships in complex data sets. PCA was conducted using Direct Oblimin rotation with Kaiser Normalization.

2.6. Catchment and Ice Sheet P Fluxes

2.6.1. Dissolved Fluxes of P

Catchment meltwater fluxes for the sampled years (2012 and 2013) were calculated from the seasonal discharge record following the method of Cowton *et al.* [2012]. Total catchment runoff was derived by summing discharge from each 5 or 10 min data point (frequency at which discharge was logged) over the monitoring period (LG = days 134–251; KS = days 112–223). Dissolved P fluxes were calculated from the product of the water flux and the discharge-weighted mean concentrations of SRP and DOP (see section 2.4), following previous work [e.g., Meybeck, 1982; Hawkins *et al.*, 2014]. A P flux range was also calculated from total water flux and minimum and maximum recorded P concentrations.

Dissolved P fluxes from the GrIS were estimated from the minimum, discharge-weighted mean and maximum concentrations from our LG data set, multiplied by the mean 2000–2012 GrIS water flux taken from Tedesco *et al.* [2013], estimated as $437 (\pm 97) \text{ km}^3 \text{ yr}^{-1}$. A crude estimate of future fluxes was calculated from Tedesco *et al.* [2013] discharge data from 2012, a record melt year, when the meltwater flux was estimated to be 665 km^3 . We use P data from LG, rather than KS, since this is more likely to represent the hydrology of other large outlet catchments that dominate meltwater export from the GrIS (see Text S1) [Bartholomew *et al.*, 2011; Chu, 2014; Hawkins *et al.*, 2014].

2.6.2. Particulate Fluxes of P (PP)

LG and KS suspended sediment loads were calculated from suspended sediment concentrations (section 2.2) multiplied by discharge at each logged time point [Cowton *et al.*, 2012; Hawkins *et al.*, 2014]. A minimum, discharge-weighted mean, and maximum concentration for each PP phase ($\mu\text{g g}^{-1}$ dry sediment; section 2.4.2) was combined with sediment flux data to derive fluxes.

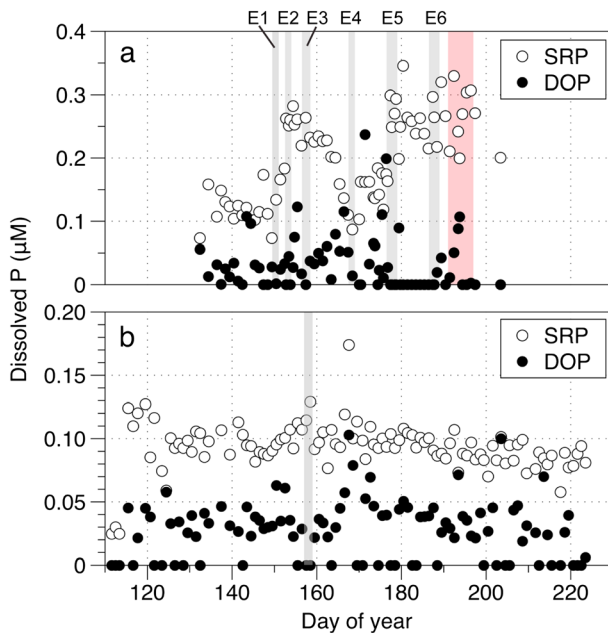


Figure 3. Time series of dissolved phosphorus species from the proglacial rivers of (a) Leverett Glacier (2012) and (b) Kiattuut Sermiat (2013). Values given as 0 are below the methodological detection limit. Grey shaded areas in Figure 3a are indicative of outburst events (E) and in Figure 3b of a significant hydrological shift in the glacial drainage system (a spring event). The red shaded area in Figure 3a highlights the 2012 record melt event.

Seasonal evolution of efficient drainage allows progressively more remote regions of the bed to be accessed. A large, well-documented, melt event was observed at LG during 2012, when over 90% of the GrIS surface was at melting point (day 194; Figure 2a) [Nghiem et al., 2012], corresponding with a record discharge of $>800 \text{ m}^3 \text{ s}^{-1}$. The melt season is interspersed with meltwater pulse events (E1–E6; Figure 2a) where discharge, suspended sediment, and EC spikes occur in response to surface lake drainage events, forcing stored waters from the glacier bed [Bartholomew et al., 2011]. Suspended sediment concentrations are high throughout, with a mean concentration of $>1.1 \text{ g L}^{-1}$ (Table 1) [Cowton et al., 2012].

KS discharge increases with supraglacial snow and ice melt throughout the ablation season, similar to LG and other temperate glaciers studied [Collins, 1979; Swift et al., 2005]. A spike in suspended sediment concentration, coupled with a sharp decline in EC and major ion concentration, accompanies a large increase in discharge and pH around day 157 (Figure 2b). This indicates the evolution of an efficient drainage system able to route water to the margin more rapidly [Mair et al., 2003], as the waters exiting the glacier are representative of those with a lower residence time (less concentrated, higher pH). Supraglacial lakes in Greenland do not form at the elevation range on which KS lies (~ 100 – 650 m above sea level); hence, there are no associated meltwater pulse events, and seasonal trends largely reflect incident supraglacial melt rates. Suspended sediment concentrations are generally lower than other glaciers, suggesting that settling in the proglacial lake may be a sink of sediments [Bagshaw et al., 2014; Liermann et al., 2012] and/or that KS glacier physical erosion rates are low due to the slow velocity (Table 1).

3.2. Dissolved Phosphorus Concentrations in Meltwaters

Elevated SRP concentrations are closely aligned with the flushing of stored waters from the subglacial system by supraglacial lake drainage events and subsequent drainage of subglacial waters from newly connected parts of the ice sheet bed (E2, E3, E5, and E6; Figure 3a). Maximum concentrations of SRP (up to $0.35 \mu\text{M}$) were recorded toward the end of the monitoring period. These are associated with the E5 and E6 events, the 2012 record melt event, and waters with a pH >9 (Figures 2a, 3a, and 4a). DOP concentrations at LG are significantly lower than SRP (Table 2 and Figure 3). DOP contributes $<10\%$ of the dissolved flux, and there is little temporal trend, with values

Sediment fluxes from the GrIS are poorly constrained but are likely globally significant [Cowton et al., 2012; Hay, 1998; Hudson et al., 2014; Jeandel and Oelkers, 2015; Lisitzin, 2002]. We use minimum (0.643 g L^{-1}), discharge-weighted mean (1.109 g L^{-1}) and maximum (3.876 g L^{-1}) suspended sediment concentrations measured at LG to derive estimates of sediment fluxes, as per Hawkins et al. [2014]. GrIS sediment yields are calculated by multiplying these values with the meltwater flux from Tedesco et al. [2013]. This method generates sediment fluxes of 0.28, 0.48, and 1.69 Gt yr^{-1} . We combine these sediment fluxes with the discharge-weighted mean PP phases from LG to derive a range of estimates (see section 2.6.1) [Hudson et al., 2014].

3. Results

3.1. Glacier Hydrology

The hydrology of LG is well studied [Bartholomew et al., 2011; Chandler et al., 2013; Cowton et al., 2013].

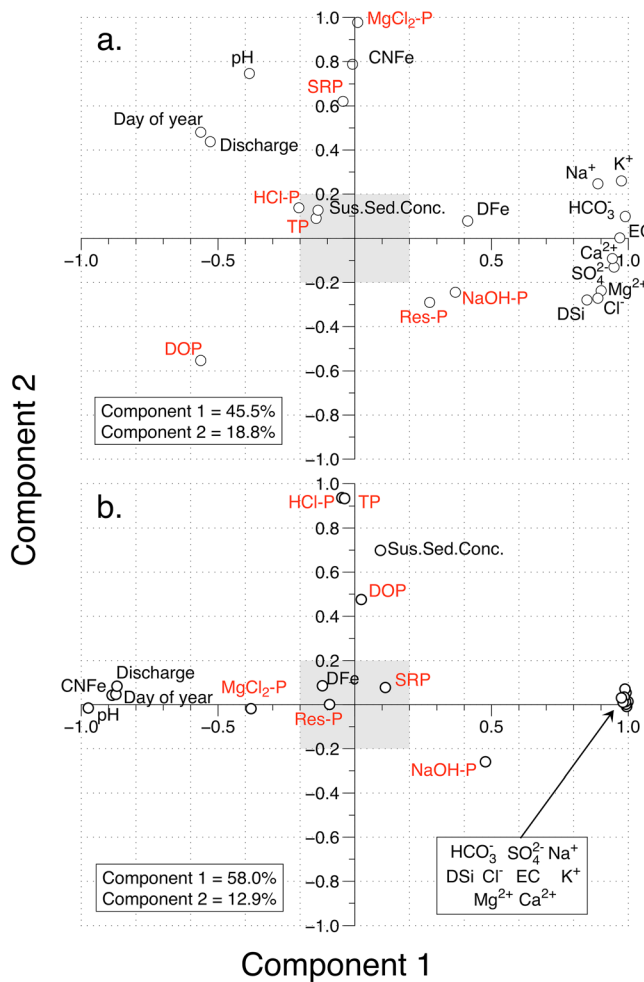


Figure 4. Principle components analysis for geochemical variables at (a) Leverett Glacier (LG) and (b) Kiattuut Sermiat (KS). Phosphorus fractions are highlighted in red. The x axis is component 1, responsible for most variance in the data set. The y axis is component 2, responsible for the second most variance in the data set. For LG and KS these components explain 64.3% and 70.9% of the variance, respectively. The amount of variance for each component is displayed in Figures 4a and 4b. Clustering of variables indicates high intercorrelation. Insignificant variables (values between +0.2 and -0.2) for components 1 and 2 are highlighted in the grey shaded box.

rocks such as basalt generally have higher P concentrations (~1000 ppm) than shield rocks (~700 ppm) [Porder and Ramachandran, 2013]. The majority (>97%) of particulate phosphorus is in the HCl-P fraction, as with LG. Labile and residual phases contributed less than at LG, <1% and ~2%, respectively.

3.4. Catchment Phosphorus Yields

We used catchment-normalized P yields [Föllmi *et al.*, 2009] to compare the efficiency of P weathering in GrIS glacial catchments compared to nonglacial rivers. SRP yields from LG and KS were high and estimated at 26.8 (8.5–43.3) and 16.7 (5.6–33.3) kg km⁻² yr⁻¹, respectively (Table 4). There is significant variation in catchment labile PP yields (Table 4). These differences (57.3 versus 8.3 kg km⁻² yr⁻¹ for LG and KS, respectively) are driven mainly by contrasting suspended sediment loads (Table 1), as extractable concentrations are of similar magnitude. Similarly, the LG TP yield (3250 kg km⁻² yr⁻¹) is nearly 4 times higher than the KS TP yield (859 kg km⁻² yr⁻¹; Table 4).

3.5. Flux Estimates

Fluxes of bioavailable P at LG change throughout the ablation season (Figure 5). Periods of enhanced P export coincide with outburst events or the extreme melt event of 2012 (days 192–197), with the highest flux

close to those of the supraglacial meltwaters we measured (Table 2), indicating a supraglacial source [Stibal *et al.*, 2008].

KS discharge-weighted mean SRP concentrations are less than LG (0.09 versus 0.23 µM; Table 2 and Figure 3b), despite the generally more concentrated waters (EC of 26.6 versus 8.5 µS cm⁻¹; Table 1). There is little temporal trend, unlike major ion concentrations (Figure 2b), and no significant loading of SRP with other variables (Figure 4). Bulk meltwater DOP concentrations are similar to supraglacial DOP concentrations, indicating a supraglacial source, as with LG.

3.3. Particulate Phosphorus Concentrations in Meltwaters

The mean PP content of LG suspended sediments (850 µg g⁻¹) is similar to that measured in shield rocks (Table 3) [Hodson *et al.*, 2004; Porder and Ramachandran, 2013]. The majority (>90%) of the PP is HCl extractable and is believed to be predominantly fluorapatite. Labile PP (MgCl₂ + NaOH extractable) accounts for ~2% of total PP, with the majority extracted as NaOH-P (P bound to amorphous Fe; Table 3). Around 4% of extractable P is present as residual P. KS suspended sediments contain more total phosphorus than LG (~1200 µg g⁻¹; Table 3). The higher P content is likely due to the catchment geology, which although similar to LG, includes basaltic intrusions. Basic

Table 2. Mean Dissolved Phosphorus Concentrations From Glacial Study Sites and Arctic Rivers^a

Study Area	Type	SRP	DOP	n	Source
		($\mu\text{M P L}^{-1}$)			
<i>Glacial Study Sites</i>					
Greenland					
Leverett Glacier	Runoff	$0.23^{\text{b}} \pm 0.07$	$0.03^{\text{b}} \pm 0.04$	77	This study
Kiattuut Sermiat	Supraglacial	<LoD			Telling et al. [2012]
	Runoff	$0.09^{\text{b}} \pm 0.02$	$0.03^{\text{b}} \pm 0.03$	104	This study
Antarctica	Supraglacial	<0.01	0.04		This study
Onyx River	Runoff	0.14		22	Green et al. [2005]
Taylor Glacier	Supraglacial	0.18			Mueller et al. [2001]
Canada Glacier	Cryoconite hole	0.10	0.19		Telling et al. [2014]
Commonwealth Glacier	Cryoconite hole	0.19		22	Bagshaw et al. [2013]
Svalbard					
Austre Broggerbreen	Runoff	<LoD			Hodson et al. [2005]
Midre Lovenbreen	Cryoconite hole	0.12			Anesio et al. [2007]
	Runoff	0.03			Mindl et al. [2007]
Werenskioldbreen	Cryoconite hole	0.12			Anesio et al. [2007]
	Runoff	0.03	0.18		Stibal et al. [2008]
Europe	Supraglacial	0.02	0.20		
Rhone Glacier ^c	Runoff	0.05	0.05	64	Föllmi et al. [2009]
Oberaar Glacier ^c	Runoff	0.08	0.07	49	
Americas					
Mendenhall River ^d (Alaska) ^d	Runoff	0.31 ± 0.25		14	Hood and Berner [2009]
White Glacier (Canadian high Arctic)	Supraglacial	0.08			Mueller et al. [2001]
Upper Manso Glacier (Patagonia)	Runoff	0.14 ± 0.09		3	Chillrud et al. [1994]
<i>Arctic Rivers</i>					
Mackenzie River		0.06			Telang et al. [1991]
Mackenzie River		0.03	0.04		Emmerton et al. [2008]
Yukon River		0.05 ± 0.04	0.1 ± 0.13		Guo et al. [2004]
Alaskan rivers ^e		0.16			McClelland et al. [2014]
Russian rivers ^f		0.25 ± 0.18			Lobbes et al. [2000]
Arctic		0.07			Meybeck [1982]
(Sub)arctic		0.27 ± 0.21	0.90 ± 0.56		
Arctic ^g		0.35 ± 0.41			Le Fouest et al. [2013]
Global river mean		0.32	0.32^{h}		Meybeck [1982]

^aAll concentrations to two decimal places.^bDischarge-weighted mean concentration.^cMeasurements during ablation season.^dData from summer ablation season (May–September). Estimated from graph.^eMean SRP concentration from three Alaskan rivers.^fData from 12 Russian Arctic rivers.^gBased on discharge-weighted mean summer concentrations (May–August).^hAuthor acknowledges DOP measurements may be significant overestimates due to lack of data and methodological differences.

period occurring during the latter. This demonstrates the importance of increased meltwater input into the subglacial system as a mechanism of enhancing the P flux [Hawkins et al., 2015]. KS P fluxes are fairly consistent after the distinct hydrological change on day 157 (Figure 5). Fluxes, ranging from 0.1 to 0.3 g s^{-1} , are nearly 2 orders of magnitude lower than LG, with dissolved fluxes more important than particulate fluxes.

We use our data to estimate annual P fluxes from LG, KS, and the GrIS (Table 5). The mean annual dissolved flux from LG totaled 18.3 Mg yr^{-1} , with SRP the dominant form ($\sim 90\%$). Labile PP accounted for 34.4 (12.5 – 84.7) Mg yr^{-1} , approximately twice the SRP flux. The total P flux is estimated to be 1986 Mg yr^{-1} . KS fluxes are $<10\%$ those of LG, with estimated dissolved P export of 0.8 (0.2 – 2.5) Mg yr^{-1} , largely due to lower annual

Table 3. Particulate Phosphorus Concentrations for Suspended Sediments From Glacial Study Sites and Major Rivers

Study Area	MgCl-P	NaOH-P	HCl-P	Res-P/POP	PP	n	Source
<i>Glacial Study Sites</i>							
Greenland							
Leverett Glacier	0.5 ± 0.4	14.6 ± 7.5	800 ± 90	34.0 ± 7.5	849 ± 97	25	This study
Kiattuut Sermiat	0.1 ± 0.1	11.9 ± 3.2	1175 ± 112	21.9 ± 3.7	1209 ± 111	25	This study
Antarctica							
Canada Glacier ^a	0.5	10.3			1455	8	Telling et al. [2014]
Commonwealth Glacier ^a	0.28	33.5	140	288	462	5	Bagshaw et al. [2013]
Canada Glacier ^a	0.41	6.67	115	259	381	18	Bagshaw et al. [2013]
Taylor Glacier ^a	0.86	6.98	95.3	367	470	5	Bagshaw et al. [2013]
Svalbard							
Austre Broggerbreen		3.5 ^b 2.4 ^{b,c}			400 460 ^c	11 6	Hodson et al. [2004]
Midre Lovenbreen		2.5 ^b 0.9 ^{b,c}			460 470 ^c	34 3	Hodson et al. [2004]
Werenskioldbreen ^a	4.8	139	440	1628	2200		Stibal et al. [2008]
Europe							
Rhone Glacier (Swiss Alps)		21.8 ^d	315	8.4	375	23	Föllmi et al. [2009]
Oberaar Glacier (Swiss Alps)		52.0 ^d	579	16.8	618	9	Föllmi et al. [2009]
Storglaciären (Sweden)		23 ^{b,c}			670 ^c	4	Hodson et al. [2004]
Glacier du Trient (French Alps)		1.6 ^{b,c}			230 ^c	4	Hodson et al. [2004]
Asia							
Batura (Pakistan)		1.1 ^{b,c}			400 ^c	4	Hodson et al. [2004]
<i>Major Rivers for Comparison</i>							
Mississippi	337	469 ^d	115 ^d	62 ^d	1085	34	Sutula et al. [2004]
Amazon		217 ^{b,d}	217 ^d	217 ^d	651	4	Berner and Rao [1994]
Changjiang (Yangtze)	37.8	30.8 ^d	193 ^d	175 ^d	817		Meng et al. [2015]

^aCryoconite sediment.^bIncludes MgCl₂-P extraction.^cProglacial sediment.^dApproximations—different extraction technique to that used in this study.

discharge. The KS labile PP flux is lower than the dissolved P (DP) flux, at 0.3 (0.1–0.5) Mg yr⁻¹ (Table 5). Only a small fraction of total P export from KS is “labile,” with most exported as more refractory phosphorus in sediments. Our flux estimates indicate that PP dominates the P flux from LG and KS (>97%). PP therefore dominates export from the GrIS; we estimate that 408 (238–1436) Gg Pyr⁻¹ is discharged into the surrounding coastal regions annually. The most highly reactive labile fractions are estimated to account for 10.9 (5.3–34.0) Gg Pyr⁻¹, with dissolved fractions comprising ~33%.

4. Discussion

4.1. Catchment Comparison

There are clear differences in the P cycle at LG and KS. Catchment hydrology likely exerts a first-order influence on phosphorus concentrations since LG and KS bedrock is similarly composed of igneous crystalline rock geology. Concentration of bedrock P is elevated at KS (Table 3); thus, if catchment hydrology were similar, one would expect elevated concentrations at KS. Catchment size, and hence meltwater residence time, therefore appears to be an important factor in dictating SRP concentration where bedrock geology is relatively uniform [Wadham et al., 2010]. More remote regions farther from efficient drainage pathways are likely at the bed of the larger LG, allowing longer-term storage of subglacial waters. In comparison, the bed of the smaller KS is likely to be extensively flushed each year due to the closer proximity of waters to efficient drainage pathways. We therefore hypothesize that the higher concentrations of SRP at LG are the result of longer residence time waters, giving rise to enhanced biogeochemical weathering of bedrock. This hypothesis is likely to hold true for PP species as LG sediments have higher concentrations of labile phases.

Mechanisms of release also differ between LG and KS (section 3.1). Elevated P fluxes at LG are associated with subglacial outburst events (E1–E6) or extreme melt periods (Figure 5) and are often sustained following such

Table 4. Phosphorus Fraction Yields From Glaciers, Arctic Rivers and Major Rivers

Study Area	Catchment Size (km ²)	Annual Runoff (km ³)	SRP	DOP	Labile PP ^a	TP	Source
			(kg P km ⁻²)				
<i>Glaciers</i>							
Greenland							
Leverett Glacier	600	2.2	26.8	3.7	57.3	3,252	This study
Kiattuut Sermiat	36	0.22	16.7	5.6	8.3	859	
Svalbard							
Austre Broggerbreen	11.8	0.03 ^b			0.48	64	Hodson et al. [2004]
Midre Lovenbreen	6.4	0.015	2.34		8.2	2,000	Mindl et al. [2007] and Stibal et al. [2008]
Werenskioldbreen	27	0.05	1.48	10.6			Stibal et al. [2008]
Europe							
Rhone Glacier (Swiss Alps)	19.1	0.08 ^b	1.99		11.7 ^c	185	Föllmi et al. [2009]
Oberaar Glacier (Swiss Alps)	6.3	0.02 ^b	2.12		31.2 ^c	389	
Storglaciären (Sweden)	6.2	0.01 ^b			42.6	1240	Hodson et al. [2004]
North America							
Lemon Creek ^d	59	0.1	30				Hood and Scott [2008]
Mendenhall River ^d	231	1	40				
<i>Rivers</i>							
Arctic rivers							
Indigirka ^e	305,000	50.4	0.8		8.7 ^f	21.9	Guo et al. [2004], Harrison et al. [2010], and Hay [1998]
Kolyma ^e	526,000	70.8	0.8		2.1 ^f	5.2	
Lena ^e	2,430,000	533	0.9		1.7 ^f	4.3	
Mackenzie ^e	1,787,000	308	0.7		9.2 ^f	22.9	
Ob ^e	2,950,000	404	10.0		1.4 ^f	3.4	
Pechora ^e	312,000	135	14.7		5.3 ^f	13.3	
Northern Dvina ^e	348,000	106	4.6		3.0 ^f	7.4	
Yana ^e	224,000	32	0.9		9.2 ^f	23.0	
Yenisey ^e	2,440,000	577	2.1		1.6 ^f	3.9	
Yukon ^e	849,000	200	2.4		21.3 ^f	53.2	
Sagavanirktoq	12,580	1.6	0.5				McClelland et al. [2014]
Kuparuk	8,107	1.3	0.7				
Colville	59,756	19.7	2.1				
Chena	5,200	1.18	1.5	0.6		6.5	Cai et al. [2008]
Major rivers							
Mississippi	2,900,000 ^g	380	14.4 ^h		92.1	124	Sutula et al. [2004]
Amazon ⁱ	6,112,000 ^g	6,300	11.9	5.1	28.5	86.3	Berner and Rao [1994]
Changjiang ⁱ	1,808,000 ^g	928	7.2		18.7	194	SRP—Zhang et al. [2003]; PP—Meng et al. [2015]
Irrawaddy	406,000	428				300	PP—Beusen et al. [2005]
Ganges	1,050,000 ^g	971				200	PP—Beusen et al. [2005]
World average	N/A		0.5			69.3	Harrison et al. [2010]; PP—Beusen et al. [2005]
			4.5				Meybeck [1982]

^aMgCl₂-P and NaOH-P extractable.^bEstimated discharge from data presented in Bogen and Bonsnes [2003] (Austre Broggerbreen), Föllmi et al. [2009] (Rhone and Oberaar glaciers), and Hock and Noetzli [1997] (Storglaciären).^cApproximations—different extraction technique to that used in this study.^dCatchment extent from Hood and Berner [2009]. Discharge and SRP yields estimated from graphs.^eCatchment extent and discharge from Harrison et al. [2010].^fAssumption that ~40% PP is labile P.^gFrom Harrison et al. [2010].^hIncludes both SRP and DOP.ⁱSediment yield data from Hay [1998].

events. These hydrological events play a critical role as they enhance fluxes in the short term and drive changes in subglacial drainage by promoting subglacial water flow from higher up catchment. This likely allows drainage of increasingly isolated regions of the subglacial system, where waters high in P are likely to exist. Hence, this drainage system evolution promotes elevated P fluxes several days after outburst events.

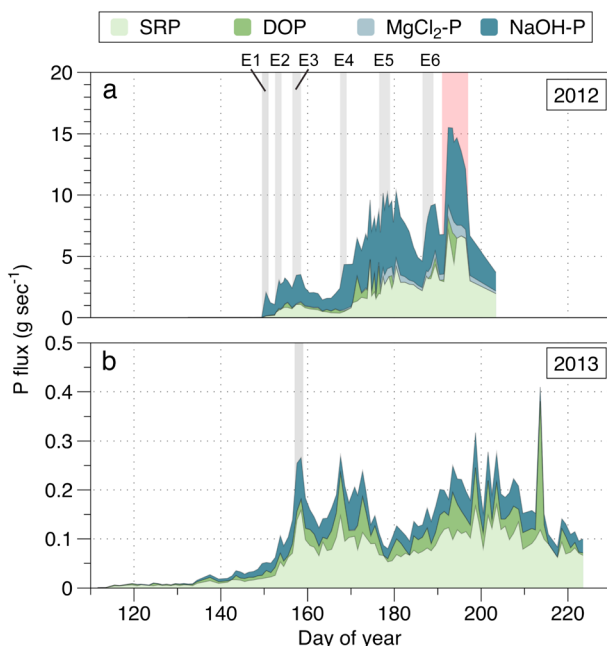


Figure 5. Time series of calculated phosphorus fluxes at (a) Leverett Glacier and (b) Kiattuut Sermia. Only “bioavailable” phosphorus fractions are shown (dissolved P phases plus MgCl₂-P and NaOH-P). Dissolved fluxes are represented with green colors, and particulates fluxes with blue/grey colors. Fluxes are cumulative at each time point. Grey shaded areas in Figure 5a are indicative of outburst events (E) and in Figure 5b of a significant hydrological shift in the glacial drainage system (a spring event). The red shaded area in Figure 5a highlights the 2012 record melt event.

the season at KS. Little change is evident after approximately day 160, as reflected in KS temporal flux records (Figure 5). Fewer isolated regions of subglacial drainage are likely to exist due to the smaller catchment size, and relatively rapid onset of efficient drainage in the ablation season, as found at Alpine glaciers [Swift *et al.*, 2005]. Supraglacial lake-induced outburst events do not occur at KS.

4.2. Controls on Phosphorus Concentrations in GrIS Meltwaters

Most dissolved P in glacial meltwaters is derived from the dissolution of P-containing rock. Both LG and KS are located on crystalline bedrock with fluorapatite by far the most dominant mineral form of P [Porder and Ramachandran, 2013]. Physical erosion of bedrock by glacier action exposes finely ground apatite to biogeochemical weathering, liberating SRP. Hence, elevated concentrations of SRP are likely to arise from glacial comminution of bedrock.

Fe appears important in the glacial P cycle at LG (Figures 6 and 7), as has been observed in nonglacial river waters [Gunnars *et al.*, 2002; Ruttenberg, 2014; Slomp, 2011]. High colloidal/nanoparticulate Fe concentrations (filterable through a <0.45 μm membrane; CNFe) were recorded at LG during this monitoring period [Hawkins *et al.*, 2014]. A significant correlation between SRP and CNFe up to CNFe concentration of 2 μM ($R^2 = 0.6$; $P < 0.01$; Figures 4 and 6) indicates sorption of SRP onto highly reactive Fe (oxy)hydroxide nanoparticles or colloids <0.45 μm in size [Froelich, 1988]. Changes in SRP and CNFe are also closely correlated to pH with concentrations highest at pH >9, where the solubility of iron (oxy)hydroxides increases (Figures 2a and 4) [Drever, 1997]. The iron (oxy)hydroxide point of zero charge is also at pH ~9. When water reaches this pH the desorption of negatively charged SRP from the iron (oxy)hydroxide surface into solution is favored. This may also explain the weaker correlation between SRP and CNFe when CNFe concentrations are >2 μM (Figure 6).

Buffering of SRP by particulate Fe fractions also appears to be important (Figures 4 and 7). There is a significant correlation between SRP and NaOH-P (Fe-bound P; $R^2 = 0.6$, $P < 0.01$; Figures 4 and 7). The MgCl₂-P phase is likely a transition between dissolved and Fe-bound P (Figure 7) [Froelich, 1988; Ruttenberg, 2014].

It is probable that seasonal P trends will change at LG with climatic warming [Hawkins *et al.*, 2015]. For example, the region of supraglacial lake formation and drainage on the GrIS is predicted to increase in a warmer climate [Leeson *et al.*, 2015], potentially leading to a higher incidence of outburst events in the catchment. Furthermore, high P fluxes may initiate earlier, with elevated P fluxes continuing until later, as the melt season grows in length and intensity. Conversely, over time more regular flushing may lower bioavailable P concentrations, as the residence time of stored waters falls. There is large uncertainty in the response of suspended sediment flux to enhanced warming, as little data are currently available [Cowton *et al.*, 2012; Hawkins *et al.*, 2015; Hudson *et al.*, 2014]. Changes to suspended sediment dynamics will have a large impact on fluxes of PP downstream. Evidence from past deglaciation events suggests that sediment fluxes may increase in the future [Jeandel and Oelkers, 2015].

An efficient, channelized drainage system is established fairly early in

Table 5. Phosphorus Flux Estimates From Leverett Glacier and Kiattuut Sermiat, With Scaled Estimates for Greenland Ice Sheet Meltwater Runoff^a

P Source	Water/Sediment Flux ^b	Min	Mean	Max	Source
		(P flux per year)			
Leverett Glacier (Mg)					
SRP ^c	2.20 km ³ yr ⁻¹	5.1	16.1	26.0	This study
DOP ^c		0.0	2.2	16.1	
Labile PP ^d	2.31 Tg yr ⁻¹	12.5	34.4	84.7	
TP ^d		1,617	1,986	2,697	
Kiattuut Sermiat (Mg)					
SRP ^c	0.22 km ³ yr ⁻¹	0.2	0.6	1.2	This study
DOP ^c		0.0	0.2	1.3	
Labile PP ^d	0.02 Tg yr ⁻¹	0.1	0.3	0.5	
TP ^d		27.7	30.9	36.9	
Greenland Ice Sheet (2000–2012) (Gg)					
SRP ^e	437 km ³ yr ⁻¹	1.0	3.2	5.2	This study
DOP ^e		0.0	0.4	3.2	
Labile PP ^f	300–1700 Tg yr ⁻¹	4.3	7.3	25.6	
TP ^f		238	408	1,436	
Greenland Ice Sheet (2012) (Gg)					
SRP ^e	665 km ³ yr ⁻¹	1.5	4.9	7.8	This study
DOP ^e		0.0	0.7	4.9	
Labile PP ^f	400–2600 Tg yr ⁻¹	6.5	11.1	39.0	
TP ^f		363	620	2,186	
<i>Atmospheric Deposition</i>					
Global (Gg)		96.5			
Labile PP ^g		560.0			Mahowald et al. [2008]
TP					
Arctic					
Labile PP ^g		2.2			Mahowald et al. [2008]
TP		6.9			
<i>Rivers</i>					
Arctic ^h (Gg)					
SRP ⁱ	2400 km ³ yr ⁻¹	3.9	19.5	51.7	Guo et al. [2004], Holmes et al. [2012], and Le Fouest et al. [2013]
DOP ⁱ		3.9	19.5	51.7	
Labile PP ^j	220 Tg yr ⁻¹	12.6	31.4	50.2	Guo et al. [2004], Meng et al. [2015], and Ruttenberg [2014]
TP ^j		126			
Amazon ^h (Gg)					
SRP	6590 km ³ yr ⁻¹	79.1			Berner and Rao [1994]
DOP		33			
Labile PP	734 Tg yr ⁻¹	159			
TP		475			
Mississippi ^h (Gg)					
SRP	528 km ³ yr ⁻¹	40.9			Sutula et al. [2004]
DOP		9			
Labile PP	333 Tg yr ⁻¹	268			
TP		361			
Changjiang ^h (Gg)					
SRP	928 km ³ yr ⁻¹	13.0			Meng et al. [2015] and Zhang et al. [2003]
DOP ^k		13.0			
Labile PP	463 Tg yr ⁻¹	33.6			
TP		347			
Global (Gg)					
SRP		310		770	Ruttenberg [2014]
DOP		310		770	
Labile PP		1,828	4,801	8,053	Meng et al. [2015] and Ruttenberg [2014]

Table 5. (continued)

P Source	Water/Sediment Flux ^b	Min	Mean	Max	Source
	(P flux per year)				
TP	18,275	19,204	20,133		Ruttenberg [2014]
^a Estimates of atmospheric phosphorus fluxes and riverine phosphorus fluxes are also given.					
^b Water and sediment flux are presented as $\text{km}^3 \text{yr}^{-1}$ and Tg yr^{-1} , respectively.					
^c Derived from minimum, discharge-weighted mean, and maximum concentrations as respective glaciers multiplied by glacier meltwater flux.					
^d Derived from minimum, discharge-weighted mean, and maximum labile PP concentrations ($\text{MgCl}_2\text{-P} + \text{NaOH-P}$) at respective glaciers multiplied by glacier suspended sediment flux.					
^e Derived from minimum, discharge-weighted mean, and maximum concentrations at LG multiplied by GrIS meltwater flux [Tedesco <i>et al.</i> , 2013].					
^f Derived from minimum (0.643 g L^{-1}), discharge-weighted mean (1.109 g L^{-1}), and maximum (3.876 g L^{-1}) suspended sediment concentrations, and the discharge-weighted mean labile PP concentrations ($\text{MgCl}_2\text{-P} + \text{NaOH-P}$) at LG (see Table 3; as in Hawkins <i>et al.</i> [2014]).					
^g Estimated solubility of P in mineral aerosols is taken as labile P concentration.					
^h Using discharge from Harrison <i>et al.</i> [2010] and sediment flux from Hay [1998].					
ⁱ Derived from a minimum SRP value observed by Guo <i>et al.</i> [2004] and a maximum SRP from Le Fouest <i>et al.</i> [2013]. Mean value is derived from Holmes <i>et al.</i> [2012], assuming ~50% of measured DP is SRP and ~50% is DOP. Minimum and maximum DOP values are assumed to be ~50% of DP [Ruttenberg, 2014].					
^j Using total P data from Guo <i>et al.</i> [2004] or Ruttenberg [2014] as indicated by "source." Due to lack of data, we assume that minimum, mean, and maximum labile P concentrations are 10% [Meng <i>et al.</i> , 2015], 25%, and 40% [Ruttenberg, 2014] of total PP, respectively.					
^k Due to lack of data it is assumed that ~50% of DP is DOP [Ruttenberg, 2014].					

High pH waters in the latter part of the sampling period (approximately day 170, Figure 2a), coupled to increasing SRP and $\text{MgCl}_2\text{-P}$ (Figure 7), suggest P is derived from NaOH-P. This may be linked to the higher solubility and point of zero charge of P-bearing Fe (oxy)hydroxides at $\text{pH} > 9$ [Drever, 1997].

Conversely, we infer that at KS little cycling between phases is occurring. There is no significant relationship between Fe and P, and SRP and PP. This is likely to be due to the lower concentrations of highly reactive suspended sediments for weathering, and the comparatively short water residence times of small versus large glacier systems [Wadham *et al.*, 2010]. We postulate that water residence times (in comparison with LG) are the critical control. This is consistent with observations of Fe-P relationships at other small glaciers [Föllmi *et al.*, 2009; Hodson *et al.*, 2004], attributed to the relatively short residence times of waters exiting the glaciers and limited secondary Fe mineral formation.

To our knowledge, this is the first time a temporal trend in more labile PP fractions has been shown (at LG; Figure 8a). NaOH-P is high in early season sediments and generally declines toward the end of the sampling period,

while $\text{MgCl}_2\text{-P}$ does the opposite (Figure 8a). PCA for LG (Figure 4a) shows that $\text{MgCl}_2\text{-P}$ positively loads with SRP and day of year on component 2, while NaOH-P and Res-P are negatively loaded. NaOH-P and Res-P are also positively loaded on component 1, alongside major ions. There is a subtler trend at KS (Figure 4b), with significant values (taken as > 0.2 or < -0.2) on component 1 obtained for $\text{MgCl}_2\text{-P}$ (-0.379) and NaOH-P (0.478). These P species load with similar variables to LG. PP fractional concentrations are therefore closely tied to the geochemical conditions in glacial meltwaters. These temporal trends demonstrate the capacity for PP concentrations to change over relatively short timescales (days to weeks) in natural waters, such as seasonally evolving glacial meltwater runoff.

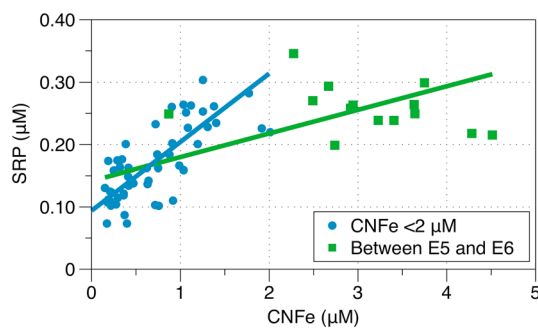


Figure 6. Relationship between SRP and CNFe (Fe filterable through a $0.45 \mu\text{m}$ membrane) for samples collected at Leverett Glacier. The green regression line ($R^2 = 0.44, P < 0.01$) is the regression of all samples. The blue regression line ($R^2 = 0.6, P < 0.01$) indicates the relationship of SRP and CNFe, where CNFe $< 2 \mu\text{M}$. Green sample points (squares) indicate samples collected between and including the E5 and E6 outburst events (days 176–189).

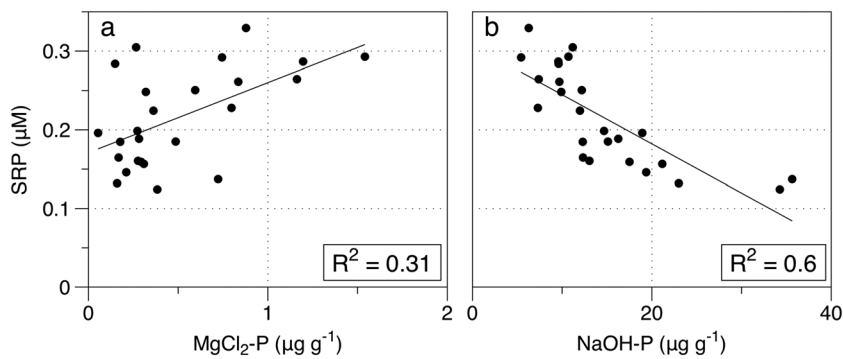


Figure 7. Relationship between SRP and labile particulate phosphorus ($\text{MgCl}_2\text{-P}$ and NaOH-P) species at Leverett Glacier. R^2 values ($P < 0.01$) for the linear regressions of SRP versus extraction are given in the bottom right of the graphs.

4.3. Comparison of GrIS Phosphorus Concentrations to Other Study Areas

4.3.1. Dissolved Species

Mean LG SRP concentrations are significantly higher than comparable glacial studies (Table 2). Only *Hood and Berner* [2009] measured higher concentrations in glacial meltwaters ($\sim 0.3 \mu\text{M}$; Table 2). KS SRP concentrations are closer to those from literature. It is difficult to compare glacial DOP concentrations due to the lack of available data. We would expect SRP to be the dominant dissolved species in glacial runoff, in agreement with *Föllmi et al.* [2009].

Leverett Glacier meltwater SRP concentrations are similar to the global weighted mean nonglacial river concentration of $0.32 \mu\text{M}$ (Table 2) [Meybeck, 1982]. Concentrations of SRP in Arctic rivers range from 0.03 to $0.35 \mu\text{M}$, with most $<0.2 \mu\text{M}$ (Table 2). DOP can account for $>50\%$ of the total DP load in nonglacial riverine waters (Table 2) [Meybeck, 1982; Ruttenberg, 2014]. DOP also likely dominates dissolved fluxes from Arctic

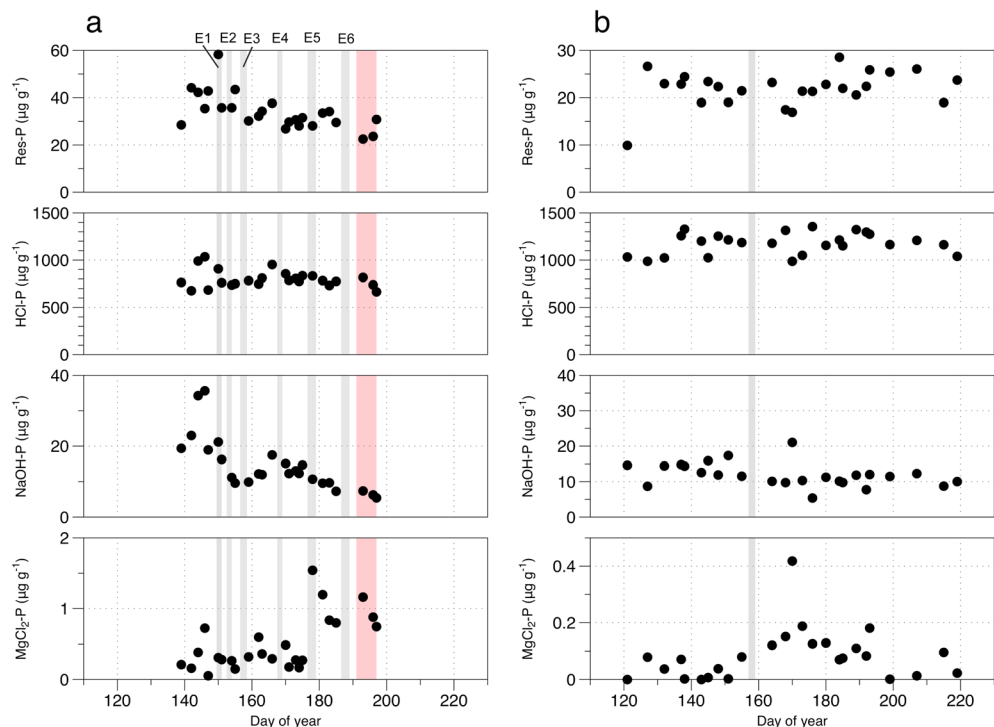


Figure 8. Time series of particulate phosphorus species from (a) Leverett Glacier and (b) Kiattuut Sermiat. Grey shaded areas in Figure 8a are indicative of outburst events (E) and in Figure 8b of a significant hydrological shift in the glacial drainage system (a spring event). The red shaded area in Figure 8a highlights the 2012 record melt event.

watercourses. For example, mean concentrations of $\sim 0.9 \mu\text{M}$ and $\sim 2.3 \mu\text{M}$ reported by Meybeck [1982] and Emmerton *et al.* [2008] in Arctic rivers are much higher than glacial meltwaters. Higher DOP is consistent with elevated dissolved organic carbon concentrations observed in (sub)arctic rivers versus glacial meltwaters [Lawson *et al.*, 2014; Lobbes *et al.*, 2000]. However, the lability of DOP is currently not well understood, and significant enzymatic processing may be required before utilization [Cotner and Wetzel, 1992; Paytan and McLaughlin, 2007].

4.3.2. Particulate Species

Hodson *et al.* [2004] presented NaOH-P (+ MgCl₂-P) data from the suspended and proglacial sediments of five valley glaciers. Values were typically much lower than those found in this study, with the exception of Storglaciären (Table 3). Föllmi *et al.* [2009] published extraction data from temperate valley glacier sediments, but the method used was different to this study, and since the phases are operationally defined, both data sets are not directly comparable. As a result, the more aggressive extraction they used for Fe-/Al-bound P may explain elevated concentrations of $20\text{--}50 \mu\text{g g}^{-1}$ versus $10\text{--}15 \mu\text{g g}^{-1}$ in this study (Table 3).

PP in glacial meltwaters appears to be significantly different in composition to PP from nonglacial rivers, although surprisingly little data are available for comparison. Riverine sediments potentially contain more labile P fractions. Specifically, organic PP comprises a much larger proportion of exported material (20–40%) [Meybeck, 1982; Ruttenberg, 2014]. Fe-/Al-bound P and mineral P (such as apatite) are generally responsible for the majority of inorganic PP ($>40\%$ of total PP) [Berner and Rao, 1994; Paytan and McLaughlin, 2007].

GrlS concentrations for Fe-bound PP phases tend to be significantly lower than those from riverine studies (Table 3). This is likely partly due to the extraction technique used. The NaOH extraction in this study is more selective for labile P (algal available) bound to the surface of Fe (oxy)hydroxides [Eijssink *et al.*, 1997; Levy and Schlesinger, 1999], while the CBD (citrate-bicarbonate-dithionite solution) method [Ruttenberg, 1992] used in a number of riverine studies [e.g., Berner and Rao, 1994; Meng *et al.*, 2015] typically gives higher estimates, because it removes more refractory Fe-P phases [Eijssink *et al.*, 1997; Golterman, 1996]. We performed an additional extraction on fresh LG suspended sediments to test this. A well-characterized ascorbate extraction for highly reactive amorphous ferrihydrite was used [Raiswell *et al.*, 2010], and $26.7 (\pm 8.9) \mu\text{g g}^{-1}$ ($n = 32$) of Fe-P was extracted versus $14.6 (\pm 7.5) \mu\text{g g}^{-1}$ for the NaOH-P extraction. This indicates that the NaOH-P extraction is selective for only the most labile Fe-P component. Our values are therefore conservative estimates compared to riverine Fe-P using the CBD method.

The organic PP content of glacial suspended sediments (Res-P) was low compared to riverine waters (Table 3). This is likely due to the low organic carbon content of LG sediments and the relative immaturity of freshly weathered subglacial debris compared to highly weathered riverine particulate matter [Lawson *et al.*, 2014].

4.4. The Greenland Ice Sheet as a “Hot Spot” of Phosphorus Denudation

4.4.1. SRP Denudation

Our results suggest that the GrlS is among the most efficient regions of P weathering and export in the world. Dissolved P yields are among the highest observed in literature (Table 2). These rates are elevated compared to those reported in other glacial catchments, apart from Hood and Scott [2008] (Table 4), where SRP yields $>30 \text{ kg km}^{-2} \text{ yr}^{-1}$ were recorded at two North American glaciated watersheds.

SRP yields from LG and KS are larger than those of nonglacial riverine catchments. They are nearly 2 orders of magnitude larger than the modeled global mean SRP denudation rate of Harrison *et al.* [2010], an order of magnitude greater than the global mean estimate of Meybeck [1982], and are similar to those reported in some of the world’s largest watersheds such as the Amazon, the Mississippi, and the Changjiang (Table 4) [Berner and Rao, 1994; Harrison *et al.*, 2010; Sutula *et al.*, 2004]. Our SRP yields are substantially higher than those from Arctic river catchments, which comprise the majority of freshwater delivery to the Arctic oceans (we estimate a discharge-weighted mean of $3.7 \text{ kg km}^{-2} \text{ yr}^{-1}$; Table 4) [Harrison *et al.*, 2010]. Even if dissolved P yields were twice these estimates (to include organic P), GrlS catchment yields would still be significantly higher. These high observed glacial SRP denudation rates are likely due to bedrock comminution exposing finely ground P minerals for weathering, and the flushing of long-term stored waters from the ice sheet bed.

4.4.2. Particulate Phosphorus Denudation

From other studies on glacial catchments only Storglaciären has comparative labile PP yields to LG (Table 4) [Hodson *et al.*, 2004]. The low yield estimated for cold-based Austre Broggerbreen (Table 4) [Hodson *et al.*, 2004]

is probably due to the absence of an active subglacial drainage system, and hence lower physical and biogeochemical weathering, demonstrating the importance of active subglacial hydrology. Differences in extraction technique mean that data from glaciers in the Swiss Alps are not directly comparable [Föllmi *et al.*, 2009], although their values lie between those of LG and KS (Table 4).

Riverine labile PP yields are comparable to GrIS catchments (Table 4), despite labile particulate phosphorus concentrations in riverine particulates tending to be much higher (Table 3) [Ruttenberg, 2014]. This is due to the lower suspended sediment loads (and by association erosional force) of rivers compared to glacial meltwaters ($<0.1 \text{ g L}^{-1}$ compared to $>1 \text{ g L}^{-1}$, respectively) [Meybeck, 1982]. We could only find measurements of PP concentrations in major Arctic rivers for the Yukon [Guo *et al.*, 2004], and for a smaller Arctic river [Cai *et al.*, 2008]. We combine Arctic river sediment yield data from Hay [1998] with discharge-weighted total PP data from Guo *et al.* [2004] ($571 \mu\text{g g}^{-1}$), and mean labile PP phase data from the Amazon and Mississippi Rivers, where by far the most extensive PP fractionation records are available for riverine environments (~40% of total PP; Table 3) [Berner and Rao, 1994; Sutula *et al.*, 2004], to derive estimates of Arctic river basin yields for comparison. We acknowledge that these estimates are crude, because they are based on values reported from temperate/tropical rivers and use a different Fe-P extraction to this study. Despite this, yields are similar to GrIS glacial catchments (Table 4). We estimate labile P yields of $1.4\text{--}21.3 \text{ kg km}^{-2} \text{ yr}^{-1}$ for the Arctic rivers, which are $<37\%$ of LG yields and similar to KS estimates.

A particularly important finding is that total P yields from LG and KS are substantially higher than all nonglaciated catchments in the literature (Table 4). LG total P yields are approximately 50 times higher than Arctic river yields and the global average of $69.3 \text{ kg km}^{-2} \text{ yr}^{-1}$ [Beusen *et al.*, 2005] and are at least an order of magnitude greater than estimates from rivers with elevated physical weathering and particulate loads, such as the Ganges, the Changjiang, and the Irrawaddy (Table 4). LG total P denudation rates also exceed estimates from other glacial catchments by ~60–1700%, while KS total P yields are similar. Thus, high rates of physical erosion and biogeochemical weathering of sediments in the subglacial environment, coupled with large annual freshwater discharge, indicate that the GrIS is a hot spot of P weathering and export in the Arctic.

4.5. Importance of Greenland Ice Sheet P Fluxes to the Arctic Oceans

We generated a labile P Arctic river flux estimate of $70.4 (20.4\text{--}153.6) \text{ Gg P yr}^{-1}$, using the methods detailed in Table 5. Atmospheric P deposition for the Arctic is taken from Mahowald *et al.* [2008]. They estimate annual Arctic Ocean atmospheric TP deposition of 6.9 Gg yr^{-1} , with 2.2 Gg solubilized to SRP (the labile fraction; Table 5). These combined P fluxes total $72.6 \text{ Gg P yr}^{-1}$; thus, we estimate meltwater runoff from the GrIS constitutes approximately 15% (10.9 Gg yr^{-1}) of the labile P flux to the Arctic oceans. More significantly, we estimate that TP fluxes from the ice sheet ($\sim 408 \text{ Gg yr}^{-1}$) are more than 3 times that of the flux from Arctic rivers ($\sim 125 \text{ Gg yr}^{-1}$) and approximately 60 times larger than atmospheric TP deposition ($\sim 7 \text{ Gg yr}^{-1}$). GrIS fluxes are similar to those of the Chianjiang, Amazon, and Mississippi Rivers (Table 5).

It has generally been observed that a fraction of sediment P is rapidly released to solution in artificial estuarine waters [Froelich, 1988]. This explains the characteristic nonconservative behavior of SRP through salinity gradients. The mineral fraction (believed to be apatite) that dominates TP export from the GrIS is not usually considered labile. However, some of the less refractory PP is likely to be solubilized in the proglacial region, and in suspended and deposited sediments in near coastal regions [Oelkers *et al.*, 2008], as glacial suspended sediments have been observed to be extremely fine and highly reactive [Brown *et al.*, 1996]. Lab experimentation suggests finely ground apatite dissolves in less than a year in seawater at 4°C [Chairat *et al.*, 2007; Jeandel and Oelkers, 2015]. Thus, we believe that the high fluxes from the GrIS could have a large effect on P availability in downstream marine ecosystems after processing.

A large majority of sediment P does not reach the open ocean in riverine systems and therefore does not play an active role in short-term biogeochemical processes. Nixon *et al.* [1996] estimate that 75% of TP from large rivers would be deposited and buried in deltas, assuming 25% is solubilized [Froelich, 1988]. It is unclear if this holds true for the GrIS, where large deltas do not exist but large fjord systems do, as there is currently no data. We acknowledge that fluxes will also depend on other physical oceanographic factors around the GrIS, which might not favor significant off-shelf export [Hopwood *et al.*, 2015]. This could significantly lower the flux of P into the open ocean, as with nonglacial regions.

Our estimates do not include the P flux from icebergs. Icebergs constitute ~60% of the GrIS freshwater flux [Bamber *et al.*, 2012], rafting fresh glacial ice melt, and entrained debris off-shelf into the open ocean [Smith *et al.*, 2013]. If we assume that iceberg-entrained debris has a similar labile PP extractable content as meltwater runoff ($\sim 10 \mu\text{g g}^{-1}$) and that the mean sediment content of icebergs is $\sim 0.5 \text{ g L}^{-1}$ [Raiswell and Canfield, 2012; Smith *et al.*, 2013], we calculate a crude flux of 3.1 Gg yr^{-1} . This value is approximately the same as the atmospheric flux to the Arctic oceans and ~5% of the estimated labile flux from Arctic rivers.

We use discharge data from 2012 as a crude indicator of how fluxes may change in a warmer climate (Table 5). These estimates indicate labile fluxes of P were enhanced by ~50% compared to the 2000–2012 mean, assuming nutrient concentrations and suspended sediment loads are roughly scalable to meltwater flux, as has been indicated in other studies [Hawkins *et al.*, 2015; Hudson *et al.*, 2014], although large uncertainties exist. The predicted increase in glacial meltwater discharge of $>100\%$ by 2100 [Fettweis *et al.*, 2013] will likely outstrip the rate of increase in riverine discharge to the Arctic oceans, which is estimated to be 18–70% during the same time period [Peterson *et al.*, 2002]. We therefore postulate that GrIS meltwater runoff may become more important to the Arctic P cycle in the future.

4.6. Importance of Findings in a Wider Context

During recent glacial maxima ice sheets have been present over much of North America and northern Europe. These ice masses discharged significant quantities of glacial meltwater and associated sediments into the oceans during the glacial period, and during initial deglaciation [Clark *et al.*, 2009]. We also hypothesize that this delivered large quantities of bioavailable phosphorus to downstream environments [Föllmi *et al.*, 2009]. The snowball Earth glaciations during the Cryogenian (720 to 635 Ma) are believed to be important in elevating phosphorus concentrations and productivity in the Precambrian oceans [Planavsky *et al.*, 2010]. This may have subsequently driven the Neoproterozoic oxygenation, and evolution of metazoan life [Planavsky *et al.*, 2010; Sahoo *et al.*, 2012]. Our results indicate that widespread glacial weathering could have supplied large quantities of bioavailable P to the ocean during these periods.

5. Summary and Conclusions

The Arctic Ocean exports large quantities of nutrients into the Pacific and Atlantic Oceans, but the sources of phosphorus are currently unclear [Torres-Valdés *et al.*, 2013]. We argue that glaciers efficiently transport large quantities of phosphorus to the surrounding coastal regions. High rates of physical erosion, combined with an abundance of meltwater at the bed of the ice sheet, drive biogeochemical weathering of phosphorus minerals. We find dissolved phosphorus yields are at least equal to some of the world's largest rivers, such as the Mississippi and the Amazon. Labile fluxes from GrIS meltwaters may constitute as much as 15% of the total Arctic riverine flux ($\sim 11 \text{ Gg P yr}^{-1}$), which has previously been considered the main source of nutrients for the surrounding ocean [Torres-Valdés *et al.*, 2013], and are significantly larger than the flux from atmospheric sources [Mahowald *et al.*, 2008]. Leverett Glacier, a large catchment of the GrIS, was found to have total phosphorus yields of over $3000 \text{ kg P km}^{-2} \text{ yr}^{-1}$, which is over an order of magnitude higher than yields from riverine catchments. The ice sheet total phosphorus flux of $\sim 400 \text{ Gg yr}^{-1}$ rivals that of the largest river systems in world. Although there are large uncertainties, we propose that fluxes are annually dynamic [Hawkins *et al.*, 2015], increasing with meltwater export under warming climate scenarios. The significance of GrIS P fluxes depends on the deposition and burial of sediments in the fjord and coastal regions. This is a large unknown as no data currently exist and should be a priority of future research. Our findings have implications for our understanding of nutrient cycling during glacial transition periods and during past snowball Earth glaciations.

References

- Anesio, A. M., B. Mindl, J. Laybourn-Parry, A. J. Hodson, and B. Sattler (2007), Viral dynamics in cryoconite holes on a high Arctic glacier (Svalbard), *J. Geophys. Res.*, 112, G04S31, doi:10.1029/2006JG000350.
- Bagshaw, E. A., M. Tranter, A. G. Fountain, K. Welch, H. J. Basagic, and W. B. Lyons (2013), Do cryoconite holes have the potential to be significant sources of C, N, and P to downstream depauperate?, *Arct. Antarct. Alp. Res.*, 45(4), 440–454, doi:10.1657/1938-4246-45.4.440.
- Bagshaw, E. A., B. Lishman, J. L. Wadham, J. A. Bowden, S. G. Burrow, L. R. Clare, and D. Chandler (2014), Novel wireless sensors for in situ measurement of sub-ice hydrologic systems, *Ann. Glaciol.*, 55(65), 41–50, doi:10.3189/2014aog65a07.
- Bamber, J., M. van den Broeke, J. Ettema, J. Lenaerts, and E. Rignot (2012), Recent large increases in freshwater fluxes from Greenland into the North Atlantic, *Geophys. Res. Lett.*, 39, L19501, doi:10.1029/2012GL052552.
- Bartholomew, I., P. Nienow, D. Mair, A. Hubbard, M. A. King, and A. Sole (2010), Seasonal evolution of subglacial drainage and acceleration in a Greenland outlet glacier, *Nat. Geosci.*, 3(6), 408–411, doi:10.1038/ngeo863.

Acknowledgments

This research is part of the UK Natural Environment Research Council, NERC-funded DELVE (NERC grant NE/I008845/1) and associated NERC PhD studentship to J.H. A.T. was funded by a NERC studentship and MOSS scholarship. P.N. was supported by grants from the Carnegie Trust for University of Scotland and the University of Edinburgh Development Trust. Additional support was provided by the Leverhulme Trust, via a Leverhulme research fellowship to J.L.W. We thank all of those who assisted with fieldwork at LG and KS, as well as technical staff in LOWTEX laboratories at the University of Bristol. The data used in this article are available from the corresponding author (jon.hawkins@bristol.ac.uk) upon request. We are grateful to our anonymous reviewers for their constructive comments on the manuscript.

- Bartholomew, I., P. Nienow, A. Sole, D. Mair, T. Cowton, S. Palmer, and J. Wadham (2011), Supraglacial forcing of subglacial drainage in the ablation zone of the Greenland ice sheet, *Geophys. Res. Lett.*, 38, L08502, doi:10.1029/2011GL047063.
- Berner, R. A., and J. L. Rao (1994), Phosphorus in sediments of the Amazon River and estuary—Implications for the global flux of phosphorus to the sea, *Geochim. Cosmochim. Acta*, 58(10), 2333–2339, doi:10.1016/0016-7037(94)90014-0.
- Beusen, A. H. W., A. L. M. Dekkers, A. F. Bouwman, W. Ludwig, and J. Harrison (2005), Estimation of global river transport of sediments and associated particulate C, N, and P, *Global Biogeochem. Cycles*, 19, GB4S05, doi:10.1029/2005GB002453.
- Bhatia, M. P., E. B. Kujawinski, S. B. Das, C. F. Breier, P. B. Henderson, and M. A. Charette (2013), Greenland meltwater as a significant and potentially bioavailable source of iron to the ocean, *Nat. Geosci.*, 6(4), 274–278, doi:10.1038/ngeo1746.
- Bogen, J., and T. E. Bonsnes (2003), Erosion and sediment transport in High Arctic rivers, Svalbard, *Polar Res.*, 22(2), 175–189, doi:10.1111/j.1751-8369.2003.Tb00106.X.
- Broecker, W. S., and T. H. Peng (1982), *Tracers in the Sea*, Eldigio Press, New York.
- Brown, G. H., M. Tranter, and M. J. Sharp (1996), Experimental investigations of the weathering of suspended sediment by Alpine glacial meltwater, *Hydrol. Process.*, 10(4), 579–597, doi:10.1002/(SICI)1099-1085(199604)10:4<579::AID-HYP393>3.0.CO;2-D.
- Cai, Y. H., L. D. Guo, T. A. Douglas, and T. E. Whitledge (2008), Seasonal variations in nutrient concentrations and speciation in the Chena River, Alaska, *J. Geophys. Res.*, 113, G03035, doi:10.1029/2008JG000733.
- Chairat, C., J. Schott, E. H. Oelkers, J. E. Lartigue, and N. Harouiya (2007), Kinetics and mechanism of natural fluorapatite dissolution at 25°C and pH from 3 to 12, *Geochim. Cosmochim. Acta*, 71(24), 5901–5912, doi:10.1016/J.Gca.2007.08.031.
- Chandler, D. M., et al. (2013), Evolution of the subglacial drainage system beneath the Greenland Ice Sheet revealed by tracers, *Nat. Geosci.*, 6(3), 195–198, doi:10.1038/ngeo1737.
- Chillrud, S. N., F. L. Pedrozo, P. F. Temporetti, H. F. Planas, and P. N. Froelich (1994), Chemical-weathering of phosphate and germanium in glacial meltwater streams—Effects of subglacial pyrite oxidation, *Limnol. Oceanogr.*, 39(5), 1130–1140.
- Chu, V. W. (2014), Greenland ice sheet hydrology: A review, *Prog. Phys. Geogr.*, 38(1), 19–54, doi:10.1177/030913313507075.
- Clark, P. U., A. S. Dyke, J. D. Shakun, A. E. Carlson, J. Clark, B. Wohlfarth, J. X. Mitrovica, S. W. Hostetler, and A. M. McCabe (2009), The Last Glacial Maximum, *Science*, 325(5941), 710–714.
- Collins, D. N. (1979), Hydrochemistry of meltwaters draining from an Alpine glacier, *Arctic Alpine Res.*, 11(3), 307–324, doi:10.2307/1550419.
- Cotner, J. B., and R. G. Wetzel (1992), Uptake of dissolved inorganic and organic phosphorus-compounds by phytoplankton and bacterioplankton, *Limnol. Oceanogr.*, 37(2), 232–243.
- Cowton, T., P. Nienow, I. Bartholomew, A. Sole, and D. Mair (2012), Rapid erosion beneath the Greenland ice sheet, *Geology*, 40(4), 343–346, doi:10.1130/G32687.1.
- Cowton, T., P. Nienow, A. Sole, J. Wadham, G. Lis, I. Bartholomew, D. Mair, and D. Chandler (2013), Evolution of drainage system morphology at a land-terminating Greenlandic outlet glacier, *J. Geophys. Res. Earth Surf.*, 118, 29–41, doi:10.1029/2012JF002540.
- Death, R., J. L. Wadham, F. Monteiro, A. M. Le Brocq, M. Tranter, A. Ridgwell, S. Dutkiewicz, and R. Raiswell (2014), Antarctic ice sheet fertilises the Southern Ocean, *Biogeosciences*, 11(10), 2635–2643, doi:10.5194/bg-11-2635-2014.
- Dore, J. E., T. Houlihan, D. V. Hebel, G. Tien, L. Tupas, and D. M. Karl (1996), Freezing as a method of sample preservation for the analysis of dissolved inorganic nutrients in seawater, *Mar. Chem.*, 53(3–4), 173–185, doi:10.1016/0304-4203(96)00004-7.
- Dorich, R. A., D. W. Nelson, and L. E. Sommers (1985), Estimating algal available phosphorus in suspended sediments by chemical extraction, *J. Environ. Qual.*, 14(3), 400–405, doi:10.2134/jeq1985.00472425001400030018x.
- Drever, J. I. (1997), *The Geochemistry of Natural Waters*, 3rd ed., Prentice Hall, Upper Saddle River, N. J.
- Eijsink, L. M., M. D. Krom, and G. J. de Lange (1997), The use of sequential extraction techniques for sedimentary phosphorus in eastern Mediterranean sediments, *Mar. Geol.*, 139(1–4), 147–155, doi:10.1016/S0025-3227(96)00108-9.
- Elser, J. J., M. E. S. Bracken, E. E. Cleland, D. S. Gruner, W. S. Harpole, H. Hillebrand, J. T. Ngai, E. W. Seabloom, J. B. Shurin, and J. E. Smith (2007), Global analysis of nitrogen and phosphorus limitation of primary producers in freshwater, marine and terrestrial ecosystems, *Ecol. Lett.*, 10(12), 1135–1142, doi:10.1111/j.1461-0248.2007.01113.x.
- Emmerton, C. A., L. F. W. Lesack, and W. F. Vincent (2008), Nutrient and organic matter patterns across the Mackenzie River, estuary and shelf during the seasonal recession of sea-ice, *J. Mar. Syst.*, 74(3–4), 741–755, doi:10.1016/J.Jmarsys.2007.10.001.
- Fettweis, X., B. Franco, M. Tedesco, J. H. van Angelen, J. T. M. Lenaerts, M. R. van den Broeke, and H. Galley (2013), Estimating the Greenland ice sheet surface mass balance contribution to future sea level rise using the regional atmospheric climate model MAR, *Cryosphere*, 7(2), 469–489, doi:10.5194/tc-7-469-2013.
- Filippelli, G. M. (2008), The global phosphorus cycle: Past, present, and future, *Elements*, 4(2), 89–95, doi:10.2113/Gselements.4.2.89.
- Föllmi, K. B., R. Hosein, K. Arn, and P. Steinmann (2009), Weathering and the mobility of phosphorus in the catchments and forefields of the Rhône and Oberaar glaciers, central Switzerland: Implications for the global phosphorus cycle on glacial/interglacial timescales, *Geochim. Cosmochim. Acta*, 73(8), 2252–2282, doi:10.1016/j.gca.2009.01.017.
- Froelich, P. N. (1988), Kinetic control of dissolved phosphate in natural rivers and estuaries—A Primer on the phosphate buffer mechanism, *Limnol. Oceanogr.*, 33(4), 649–668.
- Golterman, H. L. (1996), Fractionation of sediment phosphate with chelating compounds: A simplification, and comparison with other methods, *Hydrobiologia*, 335(1), 87–95, doi:10.1007/Bf00013687.
- Grasshoff, K., K. Kremling, and M. Ehrhardt (1999), *Methods of Seawater Analysis*, 3rd ed., Wiley-VCH, Weinheim, Germany.
- Green, W. J., B. R. Stage, A. Preston, S. Wagers, J. Shacat, and S. Newell (2005), Geochemical processes in the Onyx River, Wright Valley, Antarctica: Major ions, nutrients, trace metals, *Geochim. Cosmochim. Acta*, 69(4), 839–850, doi:10.1016/J.Gca.2004.08.001.
- Gunnars, A., S. Blomqvist, P. Johansson, and C. Andersson (2002), Formation of Fe(III) oxyhydroxide colloids in freshwater and brackish seawater, with incorporation of phosphate and calcium, *Geochim. Cosmochim. Acta*, 66(5), 745–758.
- Guo, L. D., J. Z. Zhang, and C. Gueguen (2004), Speciation and fluxes of nutrients (N, P, Si) from the upper Yukon River, *Global Biogeochem. Cycles*, 18, GB1038, doi:10.1029/2003GB002152.
- Harrison, J. A., A. F. Bouwman, E. Mayorga, and S. Seitzinger (2010), Magnitudes and sources of dissolved inorganic phosphorus inputs to surface fresh waters and the coastal zone: A new global model, *Global Biogeochem. Cycles*, 24, GB1003, doi:10.1029/2009GB003590.
- Hawkins, J. R., J. L. Wadham, M. Tranter, R. Raiswell, L. G. Benning, P. J. Statham, A. Tedstone, P. Nienow, K. Lee, and J. Telling (2014), Ice sheets as a significant source of highly reactive nanoparticulate iron to the oceans, *Nat. Commun.*, 5, doi:10.1038/ncomms4929.
- Hawkins, J. R., et al. (2015), The effect of warming climate on nutrient and solute export from the Greenland Ice Sheet, *Geochem. Perspect. Lett.*, 1, 94–104, doi:10.7185/geochemlet.1510.
- Hay, W. W. (1998), Detrital sediment fluxes from continents to oceans, *Chem. Geol.*, 145(3–4), 287–323, doi:10.1016/S0009-2541(97)00149-6.

- Henriksen, N., A. K. Higgins, F. Kalsbeek, and T. C. R. Pulvertaft (2009), *Greenland From Archaean to Quaternary Descriptive Text to the 1995 Geological Map of Greenland*, 1:2 500 000, *Geol. Surv. Den. Greenl.*, vol. 18, 2nd ed., pp. 9–116, Geological Survey of Denmark and Greenland, Copenhagen.
- Hock, R., and C. Noetzli (1997), Areal melt and discharge modelling of Storglaciären, Sweden, *Ann. Glaciol.*, 24, 211–216.
- Hodson, A. J., P. Mumford, and D. Lister (2004), Suspended sediment and phosphorus in proglacial rivers: Bioavailability and potential impacts upon the P status of ice-marginal receiving waters, *Hydro. Process.*, 18(13), 2409–2422, doi:10.1002/hyp.1471.
- Hodson, A. J., P. N. Mumford, J. Kohler, and P. M. Wynn (2005), The High Arctic glacial ecosystem: New insights from nutrient budgets, *Biogeochemistry*, 72(2), 233–256.
- Holmes, R. M., et al. (2012), Seasonal and annual fluxes of nutrients and organic matter from large rivers to the Arctic Ocean and surrounding seas, *Estuaries Coasts*, 35(2), 369–382, doi:10.1007/S12237-011-9386-6.
- Hood, E., and L. Berner (2009), Effects of changing glacial coverage on the physical and biogeochemical properties of coastal streams in southeastern Alaska, *J. Geophys. Res.*, 114, G03001, doi:10.1029/2009JG000971.
- Hood, E., and D. Scott (2008), Riverine organic matter and nutrients in southeast Alaska affected by glacial coverage, *Nat. Geosci.*, 1(9), 583–587, doi:10.1038/Ngeo280.
- Hood, E., J. Fellman, R. G. M. Spencer, P. J. Hernes, R. Edwards, D. D'Amore, and D. Scott (2009), Glaciers as a source of ancient and labile organic matter to the marine environment, *Nature*, 462(7276), 1044–1047, doi:10.1038/Nature08580.
- Hood, E., T. J. Battin, J. Fellman, S. O'Neil, and R. G. M. Spencer (2015), Storage and release of organic carbon from glaciers and ice sheets, *Nat. Geosci.*, 8(2), 91–96, doi:10.1038/ngeo2331.
- Hopwood, M. J., S. Bacon, K. Arendt, D. P. Connelly, and P. J. Statham (2015), Glacial meltwater from Greenland is not likely to be an important source of Fe to the North Atlantic, *Biogeochemistry*, 124(1–3), 1–11, doi:10.1007/s10533-015-0091-6.
- Hudson, B., I. Overeem, D. McGrath, J. P. M. Syvitski, A. Mikkelson, and B. Hasholt (2014), MODIS observed increase in duration and spatial extent of sediment plumes in Greenland fjords, *Cryosphere*, 8(4), 1161–1176, doi:10.5194/Tc-8-1161-2014.
- Jeandel, C., and E. H. Oelkers (2015), The influence of terrigenous particulate material dissolution on ocean chemistry and global element cycles, *Chem. Geol.*, 395, 50–66, doi:10.1016/j.chemgeo.2014.12.001.
- Jeffries, D. S., F. P. Dieken, and D. E. Jones (1979), Performance of the autoclave digestion method for total phosphorus analysis, *Water Res.*, 13(3), 275–279, doi:10.1016/0043-1354(79)90206-9.
- Knight, P. G. (1999), *Glaciers*, 261 pp., Stanley Thornes, Cheltenham.
- Lawson, E. C., J. L. Wadham, M. Tranter, M. Stibal, G. P. Lis, C. E. H. Butler, J. Laybourn-Parry, P. Nienow, D. Chandler, and P. Dewsbury (2014), Greenland Ice Sheet exports labile organic carbon to the Arctic oceans, *Biogeosciences*, 11(14), 4015–4028, doi:10.5194/bg-11-4015-2014.
- Le Fouest, V., M. Babin, and J. E. Tremblay (2013), The fate of riverine nutrients on Arctic shelves, *Biogeosciences*, 10(6), 3661–3677, doi:10.5194/Bg-10-3661-2013.
- Leeson, A. A., A. Shepherd, K. Briggs, I. Howat, X. Fettweis, M. Morlighem, and E. Rignot (2015), Supraglacial lakes on the Greenland ice sheet advance inland under warming climate, *Nat. Clim. Change*, 5, 51–55, doi:10.1038/nclimate2463.
- Levy, E. T., and W. H. Schlesinger (1999), A comparison of fractionation methods for forms of phosphorus in soils, *Biogeochemistry*, 47(1), 25–38, doi:10.1023/A:1006105420235.
- Liermann, S., A. A. Beylich, and A. van Welden (2012), Contemporary suspended sediment transfer and accumulation processes in the small proglacial Saetrevatnet sub-catchment, Bodalen, western Norway, *Geomorphology*, 167, 91–101, doi:10.1016/J.Geomorph.2012.03.035.
- Lisitzin, A. P. (2002), *Sea-Ice and Iceberg Sedimentation in the Ocean: Recent and Past*, Springer.
- Lobbes, J. M., H. P. Fitznar, and G. Kattner (2000), Biogeochemical characteristics of dissolved and particulate organic matter in Russian rivers entering the Arctic Ocean, *Geochim. Cosmochim. Acta*, 64(17), 2973–2983, doi:10.1016/S0016-7037(00)00409-9.
- Mahowald, N., et al. (2008), Global distribution of atmospheric phosphorus sources, concentrations and deposition rates, and anthropogenic impacts, *Global Biogeochem. Cycles*, 22, GB4026, doi:10.1029/2008GB003240.
- Mair, D., I. Willis, U. H. Fischer, B. Hubbard, P. Nienow, and A. Hubbard (2003), Hydrological controls on patterns of surface, internal and basal motion during three “spring events”: Haut Glacier d’Arolla, Switzerland, *J. Glaciol.*, 49(167), 555–567, doi:10.3189/172756503781830467.
- McClelland, J. W., A. Townsend-Small, R. M. Holmes, F. Pan, M. Stieglitz, M. Khosh, and B. J. Peterson (2014), River export of nutrients and organic matter from the North Slope of Alaska to the Beaufort Sea, *Water Resour. Res.*, 50, 1823–1839, doi:10.1002/2013WR014722.
- Meng, J., Z. Yu, Q. Yao, T. S. Bianchi, A. Paytan, B. Zhao, H. Pan, and P. Yao (2015), Distribution, mixing behavior, and transformation of dissolved inorganic phosphorus and suspended particulate phosphorus along a salinity gradient in the Changjiang estuary, *Mar. Chem.*, 168, 124–134, doi:10.1016/j.marchem.2014.09.016.
- Meybeck, M. (1982), Carbon, nitrogen, and phosphorus transport by world rivers, *Am. J. Sci.*, 282(4), 401–450.
- Mindl, B., A. M. Anesio, K. Meirer, A. J. Hodson, J. Laybourn-Parry, R. Sommeruga, and B. Sattler (2007), Factors influencing bacterial dynamics along a transect from supraglacial runoff to proglacial lakes of a high Arctic glacier, *Fems Microbiol. Ecol.*, 59(2), 307–317, doi:10.1111/J.1574-6941.2006.00262.X.
- Moore, C. M., et al. (2013), Processes and patterns of oceanic nutrient limitation, *Nat. Geosci.*, 6(9), 701–710, doi:10.1038/Ngeo1765.
- Mueller, D. R., W. F. Vincent, W. H. Pollard, and C. H. Fritsen (2001), Glacial cryoconite ecosystems: A bipolar comparison of algal communities and habitats, *Nova Hedwigia*, 123, 173–198.
- Nghiem, S. V., D. K. Hall, T. L. Mote, M. Tedesco, M. R. Albert, K. Keegan, C. A. Shuman, N. E. DiGirolamo, and G. Neumann (2012), The extreme melt across the Greenland ice sheet in 2012, *Geophys. Res. Lett.*, 39, L20502, doi:10.1029/2012GL053611.
- Nixon, S. W., et al. (1996), The fate of nitrogen and phosphorus at the land sea margin of the North Atlantic Ocean, *Biogeochemistry*, 35(1), 141–180, doi:10.1007/Bf02179826.
- Oelkers, E. H., E. Valsami-Jones, and T. Roncal-Herrero (2008), Phosphate mineral reactivity: From global cycles to sustainable development, *Mineral. Mag.*, 72(1), 337–340, doi:10.1180/minmag.2008.072.1.337.
- Palmer, S., A. Shepherd, P. Nienow, and I. Joughin (2011), Seasonal speedup of the Greenland Ice Sheet linked to routing of surface water, *Earth Planet. Sci. Lett.*, 302(3–4), 423–428, doi:10.1016/J.EPSL.2010.12.037.
- Paytan, A., and K. McLaughlin (2007), The oceanic phosphorus cycle, *Chem. Rev.*, 107(2), 563–576, doi:10.1021/cr0503613.
- Peterson, B. J., R. M. Holmes, J. W. McClelland, C. J. Vorusmarty, R. B. Lammers, A. I. Shiklomanov, I. A. Shiklomanov, and S. Rahmstorf (2002), Increasing river discharge to the Arctic Ocean, *Science*, 298(5601), 2171–2173, doi:10.1126/Science.1077445.
- Planavsky, N. J., O. J. Rouxel, A. Bekker, S. V. Lalonde, K. O. Konhauser, C. T. Reinhard, and T. W. Lyons (2010), The evolution of the marine phosphate reservoir, *Nature*, 467(7319), 1088–1090, doi:10.1038/Nature09485.
- Porder, S., and S. Ramachandran (2013), The phosphorus concentration of common rocks—A potential driver of ecosystem P status, *Plant Soil*, 367(1–2), 41–55, doi:10.1007/S11104-012-1490-2.

- Raiswell, R., and D. E. Canfield (2012), The iron biogeochemical cycle past and present, *Geochem. Perspect.*, 1(1), 1–220.
- Raiswell, R., H. P. Vu, L. Brinza, and L. G. Benning (2010), The determination of labile Fe in ferrihydrite by ascorbic acid extraction: Methodology, dissolution kinetics and loss of solubility with age and de-watering, *Chem. Geol.*, 278(1–2), 70–79, doi:10.1016/j.chemgeo.2010.09.002.
- Rignot, E., and J. Mouginot (2012), Ice flow in Greenland for the International Polar Year 2008–2009, *Geophys. Res. Lett.*, 39, L11501, doi:10.1029/2012GL051634.
- Ruttenberg, K. C. (1992), Development of a sequential extraction method for different forms of phosphorus in marine-sediments, *Limnol. Oceanogr.*, 37(7), 1460–1482.
- Ruttenberg, K. C. (2014), The global phosphorus cycle, in *Treatise on Geochemistry*, edited by D. M. Karl and W. H. Schlesinger, pp. 499–558, Elsevier, Oxford.
- Sahoo, S. K., N. J. Planavsky, B. Kendall, X. Q. Wang, X. Y. Shi, C. Scott, A. D. Anbar, T. W. Lyons, and G. Q. Jiang (2012), Ocean oxygenation in the wake of the Marinoan glaciation, *Nature*, 489(7417), 546–549, doi:10.1038/Nature11445.
- Schroth, A. W., J. Crusius, I. Hoyer, and R. Campbell (2014), Estuarine removal of glacial iron and implications for iron fluxes to the ocean, *Geophys. Res. Lett.*, 41, 3951–3958, doi:10.1002/2014GL060199.
- Slomp, C. P. (2011), Phosphorus cycling in the estuarine and coastal zones: Sources, sinks, and transformations, in *Treatise on Estuarine and Coastal Science*, edited by E. Wolanski and D. McLusky, pp. 201–229, Academic Press, Waltham, doi:10.1016/B978-0-12-374711-2.00506-4.
- Smith, K. L., A. D. Sherman, T. J. Shaw, and J. Sprintall (2013), Icebergs as unique lagrangian ecosystems in polar seas, *Annu. Rev. Mar. Sci.*, 5, 269–287, doi:10.1146/Annurev-Marine-121211-172317.
- Sole, A. J., D. W. F. Mair, P. W. Nienow, I. D. Bartholomew, M. A. King, M. J. Burke, and I. Joughin (2011), Seasonal speedup of a Greenland marine-terminating outlet glacier forced by surface melt-induced changes in subglacial hydrology, *J. Geophys. Res.*, 116, F03014, doi:10.1029/2010JF001948.
- Stibal, M., M. Tranter, J. Telling, and L. G. Benning (2008), Speciation, phase association and potential bioavailability of phosphorus on a Svalbard glacier, *Biogeochemistry*, 90(1), 1–13, doi:10.1007/S10533-008-9226-3.
- Stibal, M., A. M. Anesio, C. J. D. Blues, and M. Tranter (2009), Phosphatase activity and organic phosphorus turnover on a high Arctic glacier, *Biogeosciences*, 6(5), 913–922.
- Sutula, M., T. S. Bianchi, and B. A. McKee (2004), Effect of seasonal sediment storage in the lower Mississippi River on the flux of reactive particulate phosphorus to the Gulf of Mexico, *Limnol. Oceanogr.*, 49(6), 2223–2235.
- Swift, D. A., P. W. Nienow, T. B. Hoey, and D. W. F. Mair (2005), Seasonal evolution of runoff from Haut Glacier d'Arolla, Switzerland and implications for glacial geomorphic processes, *J. Hydrol.*, 309(1–4), 133–148, doi:10.1016/J.jhydrol.2004.11.016.
- Tedesco, M., X. Fettweis, T. Mote, J. Wahr, P. Alexander, J. E. Box, and B. Wouters (2013), Evidence and analysis of 2012 Greenland records from spaceborne observations, a regional climate model and reanalysis data, *Cryosphere*, 7(2), 615–630, doi:10.5194/Tc-7-615-2013.
- Telang, S., R. Pocklington, A. Naidu, E. Romanovich, I. Gitelson, and M. Gladyshev (1991), Carbon and mineral transport in major North American, Russian arctic, and Siberian rivers: The St. Lawrence, the Mackenzie, the Yukon, the arctic Alaskan rivers, the arctic basin rivers in the Soviet Union, and the Yenisei, in *Biogeochemistry of Major World Rivers*, edited by E. T. Degens, S. Kempe, and J. E. Richey, pp. 75–104, John Wiley, Chichester.
- Telling, J., et al. (2012), Microbial nitrogen cycling on the Greenland Ice Sheet, *Biogeosciences*, 9(7), 2431–2442, doi:10.5194/bg-9-2431-2012.
- Telling, J., A. M. Anesio, M. Tranter, A. Fountain, T. Nylen, J. Hawkings, V. B. Singh, P. Kaur, M. Musilova, and J. L. Wadham (2014), Spring thaw ionic pulses boost nutrient availability and microbial growth in entombed Antarctic Dry Valley cryoconite holes, *Front Microbiol.*, 5, doi:10.3389/fmicb.2014.00694.
- Torres-Valdés, S., T. Tsubouchi, S. Bacon, A. C. Naveira-Garabato, R. Sanders, F. A. McLaughlin, B. Petrie, G. Kattner, K. Azetsu-Scott, and T. E. Whitledge (2013), Export of nutrients from the Arctic Ocean, *J. Geophys. Res. Oceans*, 118, 1625–1644, doi:10.1002/jgrc.20063.
- Tranter, M., M. Sharp, H. Lamb, G. Brown, B. Hubbard, and I. Willis (2002), Geochemical weathering at the bed of Haut Glacier d'Arolla, Switzerland—A new model, *Hydrol. Process.*, 16(5), 959–993.
- Tyrrell, T. (1999), The relative influences of nitrogen and phosphorus on oceanic primary production, *Nature*, 400(6744), 525–531, doi:10.1038/22941.
- Wadham, J. L., M. Tranter, M. Skidmore, A. J. Hodson, J. Priscu, W. B. Lyons, M. Sharp, P. Wynn, and M. Jackson (2010), Biogeochemical weathering under ice: Size matters, *Global Biogeochem. Cycles*, 24, GB3025, doi:10.1029/2009GB003688.
- Wu, J. F., W. Sunda, E. A. Boyle, and D. M. Karl (2000), Phosphate depletion in the western North Atlantic Ocean, *Science*, 289(5480), 759–762, doi:10.1126/science.289.5480.759.
- Zhang, S., H. Ji, W. Yan, and S. Duan (2003), Composition and flux of nutrients transport to the Changjiang estuary, *J. Geogr. Sci.*, 13(1), 3–12, doi:10.1007/BF02873141.